YTUP

Journal of Thermal Engineering
https://jten.yildiz.edu.tr/
https://doi.org/10.47481/jten.0023

RESEARCH ARTICLE

Evaluating the thermal performance of PV panels: an ANSYS simulation of mixed convection and air speed effects

Khaleel Saleem Jebur Al-Ogaili[1], Lina Jassim[2], Aseel Kais Rasheed[3], Muhammad Asmail Eleiwi[4], Hasan Shakir Majdi[5], Laith Jaafer Habeeb[6,*]

[1]Mechanical Department, College of Engineering, Wasit University, Kut, 52001, Iraq
[2]Mechanical Engineering Department, Mustansiriyah University, Baghdad, 10052, Iraq
[3]Scientific Research Commission, Al Jadriya, Baghdad, 10070, Iraq
[4]Electromechanical Engineering Department, College of Engineering, University of Samarra, Samarra, 34010, Iraq
[5]Department of Chemical Engineering and Petroleum Industries, Al-Mustaqbal University College, Hillah, Babylon, 51001, Iraq
[6]Training and Workshop Center, University of Technology Iraq, Baghdad, 10066, Iraq

Abstract

This work numerically examines the thermal performance of photovoltaic (PV) panels subjected to mixed convection at various external airflow velocities, simulated in ANSYS Fluent. To model solar radiation and real-time cooling capability, the panel model includes detailed, layer-specific optical and thermal properties, as well as incident solar radiation and convective cooling effects. Mesh quality and consistent numerical techniques guarantee accurate temperature estimation across PV cells. The air velocity also increased to 4 to 5 m/s, which reduced the maximum silicon cell temperature (Tmax) to 38.8 C rather than 53.3 o C, where there was a temperature drop (delta T) of 14.5 C. This cooling has been shown to have considerable impact on the performance of electrical systems. The relative power output at 5 m/s was much higher (approximately 8.1 percentage points) on the monocrystalline silicon modules at 5 m/s and a presumed temperature coefficient of power of 0.4 percent/C than at 1 m/s airflow. The layer-wise energy balance system, with a focus on reflectivity, absorptivity, and transmissivity, treats the generation of electrical energy as a heat source and therefore minimizes heat production in silicon cells. The study also outlines the boundary conditions, the turbulence model to be used in the analysis (k–ω SST), the radiation simulation, and the grid quality to enhance the validity of the numerical output. This data illustrates the significant role of convective cooling in maintaining lower temperatures in PV cells, thereby enabling higher efficiency and energy generation, particularly under conventional operating conditions that tend to cause higher temperatures and resulting performance loss. These efforts are directed towards developing a model that not only optimizes PV design but also realistically represents airflow and accounts for thermal management efficiency.

Keywords: Mixed convection, forced convection, si cell temperature, thermal management, power generation efficiency, pv system cooling.

Cite this article as: Al-Ogaili, K. S. J., Jassim, L., Rasheed, A. K., Eleiwi, M. A., Majdi, H. S., & Habeeb, L. J. (2026). Evaluating the thermal performance of PV panels: An ANSYS simulation of mixed convection and air speed effects. Journal of Thermal Engineering, 12(3), 2–21. https://doi.org/10.47481/jten.0023

1. Introduction

The temperature of photovoltaic (PV) panels greatly influences their performance; in fact, panel efficiency decreases with temperature. It is also known as the temperature coefficient of PV panels, and it indicates a decrease in the modules' power output with rising module temperature. Wind velocity and, hence, the operating temperature of PV panels are important parameters that determine heat loss from the panels. Several studies have indicated that higher wind speeds cool PV surfaces (thereby reducing module temperature) and increase module efficiency. As a case study, a study by Ibrahim et al. [1] in Calabar, Nigeria, revealed that the speed of the wind influenced the temperature of the PV modules significantly, lowering the temperature and increasing the overall production. The measured data, partially reported by Hudiiszteanu et al. (2020) [2], also showed that the stronger the wind's effect on variables such as temperature, the lower the surface temperature and the

*Corresponding Author
E-mail Adress: laith.j.habeeb@uotechnology.edu.iq

Submitted: 3 October 2025; **Accepted:** 18 October 2025

This paper was recommended for publication in revised form by Editorin-Chief Ahmet Selim Dalkılıç

Published by Yıldız Technical University, İstanbul, Türkiye
This is an open access article under the CC BY-NC license (http://creativecommons.org/licenses/by-nc/4.0/).

higher the photovoltaic system's power under variable climatic conditions. Simultaneously, Govaerts et al. (2018) [3] also explored the significance of the convective heat loss related to wind in the temperature distribution of photovoltaic modules, and the study proved that the wind cooling can drop the temperature of the module by several degrees and, accordingly, boost the efficiency of these modules in certain circumstances. Furthermore, by testing the idea of using panel orientation, namely, the angle of inclination, Kusznier (2023) [4] confirmed that it has a resolute nature in terms of controlling solar exposure and, at the same time, easing the increase in temperature. Optimal tilt angles have been proven to increase power. Along with increasing the power, other tilt angles will increase the heat gain and would decrease (sometimes significantly) efficiency (in some very hot climates). Ahmed et al. (2024) [5] report on the fabrication of phase change materials (PCMs) to increase their thermal conductivity and cool the PV panel (using iron-filled waste, IFW). The panel temperature has been reduced, and efficiency and power have increased. The efficiency of the panel has improved by 39%, with a 33% increase in power, due to the use of PCM and IFW compared to an uncooled panel. The efficiency also increased with no additional cost when using IFW. Mulford (2022) [6] indicates that in locations with high ambient temperatures, PV efficiency will be reduced by 0.5% for each 1 °C increase in ambient temperature. Hassan Z. Al Garni et al. (2022) [7] have also investigated the effect of tilt angle and orientation (with an azimuthal angle) on the efficiency of fixed PV systems across 18 locations in Saudi Arabia and compared these results with highly accurate ground measurements of irradiance. They conclude that the optimum tilts are mostly equal to the latitudes. However, the azimuths range from 20° to 53° southwest of west due to the non-uniformity of sunlight. The report further notes that an orientation changes in which semester changes lead to a 3.63% increase in yearly production, whereas the alternative semester does not, indicating that an adjustment on a semester basis is more cost-effective than monthly. The report proposes them for six different locations with this criterion. Albaha, Arar, Hail, Riyadh, Tabuk, and Taif are all highly recommended for large-scale PV use due to their high energy yield indices and suitability. Research suggests maximizing PVs in these locations for large-scale use.

It reveals that wind speed is crucial in other studies for the effectiveness of hybrid PV-wind systems. Ji and Chen (24) [8] find that areas with higher turbulence (higher wind speeds) are biased towards complementary energy yields (energy delivered) from solar and wind farms, which leads to more energy done (work) and, as a result, higher daily efficiency. The Monte Carlo simulations by Liu et al. (2023) [9] are dynamic (stochastic) calculations of the energy yield (AEP) of wind farms. The variability in the wind, the turbine model's power curve, the wind profile, and wake losses are considered. Modeling wind speed up to turbine heights and wake losses shows that the variability among turbines on flat sites is considerably low, with the largest AEP reduction (3.5%) from wake losses. Finally, uncertainty in the AEP (9%) results from the modeling approach and exceeds the error of the model that removes correlations (7.48%). This study focuses on estimating wind farms' performance and investment risks in wind farms. Irfan Jamil et al. (2023) [10] describe triple deep learning (3DL) models to predict solar photovoltaic (PV) properties (power generation, performance ratio (PR), and soiling loss) of large solar farms. In this work, the models have been tested over 25 years, using Artificial Neural Networks (ANN), Recurrent Neural Networks (RNN), and Convolutional Neural Networks (CNN), with Long Short-Term Memory (LSTM), on real data from the Quaid-e-Azam Solar Park, Pakistan. The study shows, through experimentation, that the CNN-LSTM model can predict power generation and PR more accurately than the ANN and RNN, thereby establishing CNN-LSTM as a predictive model. ANN has been found to be more suitable for predicting soiling loss. From the recent research study by Ali et al. (2025) [11], we observe that technical interventions are suggested to improve renewable energy systems, such as widely used photovoltaic (PV) panels. In line with the technique discussed above, another recent technology is proposed to solve the problem of PV panel temperature control using geothermal energy: ground-coupled heat exchangers (GHEs). Recent studies have observed that GHE-integrated PV systems are superior, as they can cool the PV panels by 20°C-25°C and are 20% more efficient in thermal and electrical performance compared to conventional PV systems.

Kara and Şahin (2023) [12] discuss the implications that climate change has on the generation of wind energy, including the change in wind spectra or the reduction in the volume of the energy. They show that although climatic conditions have changed, the region's capability, based on multi-criteria, to make use of wind energy has a positive or negative impact. This would lead to acceleration in the north and a deceleration in the Mediterranean. Hybrid solutions are to be offered to reduce the variability and improve reliability. Finally, they support further development of wind-resource forecasts using more sophisticated climate models, particularly those incorporating machine-learning approaches, to understand better the role of wind energy in a rapidly changing climate. Their findings support the need for adaptive energy planning those accounts for inherent climatic uncertainties. Similar studies conducted under desert conditions support the conclusion that the optimal tilt angle of photovoltaic (PV) panels is critical for maximizing the incident solar radiation and simultaneously reducing surface dust deposition and radiative trapping. More specifically, Sanda et al. (2025) [13] confirms that the season of the year and regions must be taken into consideration when it comes to PV tilting. The recent advances in the photovoltaic cooling systems described by Sohail et al. (2024) [14] critical analysis includes the comparison of three types of systems, which are used to decrease the panel temperatures: active, passive, and hybrid, as well as in the context of improving electrical efficiency. Forced air cooling, water-cooling systems, and nanofluid-based systems are widely used to reduce temperature, thereby optimizing efficiency. Phase-change materials (PCM) and the use of a passive heat sink are inexpensive and un-serviceable. In one of the articles, Elminshawy et al. (2023) propose a new solution for applying a floating photovoltaic (FPV) system, in which essential cooling is achieved through an angle-perforating fin (PSAPF) submerged in water and serving

as a heat sink (15). The variable of the controlled study experiment, as observed in the Mediterranean area, and external conditions, PSAPF can be used to produce greater energy and achieve reduced operating temperatures compared to a traditional FPV system. The flow of water and wind played a role in power, resulting in a 33.31 decrease in temperature and a 22-point increase in power. In addition, the PSAPF system would save the Levelized Cost of Energy (LCOE) by 17.70 percent, therefore, making it cost-effective. Overall, this research can be used to develop more effective, environmentally friendly cooling vibrations for FPV arrays. Operating temperature is one of the biggest influences on the electrical performance of photovoltaic (PV) panels: it can lower the panel's power output in both short- and long-term operation, as well as accelerate material deterioration. Wind speed, panel orientation, and ambient temperature are other mechanisms identified in most studies as affecting PV panel cooling. However, research on cooling mechanisms and their performance under isolated operational parameters has been conducted in real-world and commercial settings. Still, little attention has been paid to quantifying the relationship between the effects of mixed and forced convection on the thermal behavior of PV systems under varying air velocities in realistic commercial multi-layer installations across various operating conditions. This study aims to address this gap and systematically explore the effect of varying air velocities (from 1 to 5 m/s) on the temperature distribution and power-generation efficiency in a standard monocrystalline-silicon PV panel. The study focuses on separating and modeling the extent of forced and natural (mixed) convection effects on PV thermal regulation. Then, it analyzes an ANSYS numerical simulation solution (validated) to obtain high-resolution, layer-specific temperature profiles and correlates those profiles with panel-level output performance. As such, this work aims to identify the optimal airflow conditions that reduce harmful temperature rises in PV cells, thereby optimizing short-term operational efficiency and long-term module reliability. The proposed hypothesis is that, as air speed and forced convection increase, silicon cell temperatures will decrease, and power generation efficiency will increase compared with conditions in which natural or mixed convection predominates. The objective of this study is to provide unambiguous, evidence-based guidance for optimizing thermal management in utility-scale PV installations, to mitigate related risks, and to enable efficient, convenient integration of automated processes into such solar energy systems under increasingly demanding operating scenarios, by quantifying these mechanisms and cross-validating their application against the literature and experimental standards.

The novelty of this work lies in the use of realistic optical and thermal behavior to quantify the overall influence of mixed convection (natural plus forced) on the temperature distribution. It shows that variation in air-movement velocity from 1 to 5 m/s shifts dominance from natural to forced convection (a less-studied, nuanced regime). In the simulation, a model is used in which power generation serves as a heat sink in the thermal balance, thereby directly linking thermal management and the estimation of electrical performance. High-quality CFD modeling with precise mesh and turbulence resolution can predict temperature reductions of up to 14.5 °C under increased airflow. It links this to a possible 8.1% increase in relative electrical output. This work makes a substantial contribution to the literature in the field by combining multi-physics, detailed geometric, and material data to provide a complete thermal and electrical performance assessment that can be applied to PV panel engineering, based on simulation data, and to inform strategies for optimal cooling and lifetime tuning.

2. Materials and methods

The study focused on determining the effect of PV panels' inlet air temperature and velocity on the resulting operating temperatures under non-cooling conditions (base case). Considering the variety of PV panels on the market, a typical one is analyzed (with a power production of 1000 W). The PV panel is a monocrystalline Si-based panel containing multiple layers; the layers' sequence and physical properties are listed in Table 1. It is inclined at 45° from the horizon. The ambient air velocity varied from 1 m/s to 5 m/s in 1 m/s increments to determine the effects of air velocity on PV panel efficiency by evaluating the impact of these velocities on PV panel temperature and the effect of temperature increases on the power generated by the PV panel. Energy from solar radiation incident on the PV panel generally leaves the system either as generated power or through losses. Optical and thermal losses contribute to the latter: thermal losses arise from heat-transfer processes, including convection and radiation from the top and bottom layers to the surrounding environment, while reflective radiation from the glass (or ETFE) layer represents a significant optical loss. In addition, the generated power is included in the PV module's energy balance.

Table 1. Selected materials' physical and thermal properties

Materials	Density (kg/m^3)	Thermal Conductivity (W/(m·K))	Specific Heat Capacity (J/(kg·K))	References
ETFE	1730	0.24	1172	[16]
EVA	945	0.35	2090	[17], [18]
Silicon	2330	148	700	[19]
PET	1350	0.275	1275	[20]
CFRP	1490	6.83	1130	[21]
Tape	1012	0.19	2000	[22]

2.1. Analytical and mathematical methodology

Solar energy balance is the analytical model representing the core system approach of evaluating thermal performance that quantifies how energy enters and exits a photovoltaic (PV) system, from the moment the sun's radiation enters the system at the front surface of the module, to the final switching off and dumping of electric energy. The amount of solar influx could be denoted by Q_{solar}, the amount of solar irradiance captured by the module. In this system there are specific components defined as: Optical Losses $Q_{op,\ loss}$, the radiation reflected in the module; Thermal Losses due to the Top Surface

$Q_{th,\,loss,\,top}$ or convective and radiative transported heat within the upper module surface; and Thermal Losses due to the Bottom Surface $Q_{th,\,loss,\,bottom}$ that is convective and radiative heat transported through the bottom module surface. So, the full expression of incoming solar radiation into the energy in the PV panel, which is dissipated in the form of thermal and optical processes, and then transformed into electrical power, is described in detail in Equation 1 and Figure 1 below [20]:

$$Q_{generated} = Q_{solar} - (Q_{th,\,loss,\,top} + Q_{th,\,loss,bottom} + Q_{op,\,loss}) \quad (1)$$

Reflective losses are a notable source of future optical losses in photovoltaic (PV) setups. The amount of solar irradiance reflected from the solar-cell surface by the panel material itself is determined by the panel material's reflectance. In most PV installations, the outermost layer almost always takes one of two forms, i.e., ETFE (Ethylene Tetrafluoroethylene) or glass. That solar modules are designed with optically thick substrates means they tend to reflect a measurable fraction of the incident solar irradiance, which has the practical consequence that the power density of the irradiance on the solar cells is noticeably reduced. There is a quantitative expression that can describe this optical phenomenon, and this is explained in equation (2) below [20].

$$Q_{op,loss} = r_{ETFE} \times Q_{solar} \quad (2)$$

Where: Q_{solar} is the total incoming solar radiation, r_{ETFE} is the reflectivity of the ETFE layer. Relative reflectivity, symbolically r ETFE, is the ratio of solar radiation that does not go through a specific medium and the sun's total radiation. Therefore, a reflectivity value of 0.1 means that only 10% of the incident's irradiance is absorbed by the material, resulting in an optical energy loss in the overall energy balance.

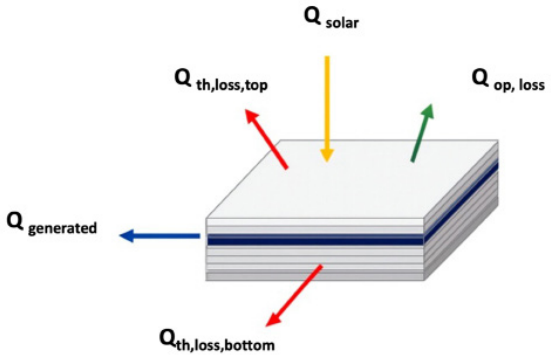

Figure 1. The distribution of the powers in the PV panel system [23]

The losses through the top surface of an individual photovoltaic (PV) module arise from two related processes: convection and radiation. Forced convection occurs when air passes over the PV surface, making it easier to remove heat from the module. Convection and radiation are the two types of thermal losses on the top surface of the PV panel. These losses flow out from the surface of the glass (ETFE), which receives the focused flux. The convection losses are a combination of free and forced convection. There is also thermal radiation loss between the glass layer and the environment; The top surface thermal losses $Q_{th,ss,top}$ can be expressed as [20]:

$$Q_{th,\,loss,top} = (Q_{Forced,\,conv,\,top} + Q_{natural,\,conv,\,top} + Q_{rad,top}) \quad (3)$$

The forced convection heat transfer coefficient, which is defined as a function of wind speed, air velocity, and module geometry, is proportional to the wind speed; therefore, a greater wind speed will result in a more significant coefficient of heat transfer and, as a result, increased heat dissipation. In contrast, natural convection occurs when the temperature of the PV panel's surface is higher than that of the surrounding environment, warming the nearby air and making it less dense, causing it to rise and pushing cooler air away. Two non-conductive processes, in combination, lead to thermal losses on the upper side of the PV module. The forced convective coefficient can be estimated from the correlation of the Nusselt number value, which is the ratio of convective to conductive heat transfer, and a dimensionless ratio with the following expression [22]:

$$Nu_{F,t} = 0.13Re\ L^{0.703}\ (1 + \sin(\beta))^{0.38} \quad (4)$$

where Re_L is the Reynolds number, used to measure the comparative magnitude of inertial and viscous forces, and β is the tilt angle of the panel. In the case of natural convection, the Nusselt number equals [22]:

$$Nu_{N,t} = 0.7386RaL^{0.1826}\ (1 + \cos(\beta))^{-0.4575} \quad \text{If } \beta \le 45° \quad (5)$$

$$Nu_{N,t} = 5.4412RaL^{0.1102}\ (1 + \cos(\beta))^{-0.085} \quad \text{If } \beta \ge 45° \quad (6)$$

Therefore, the mixed convective coefficient is calculated using the formula:

$$Nu^3_{M,t} = Nu^3_{F,t} + Nu^3_{N,t} \quad (7)$$

Where Ra_L is the intensity of buoyancy-driven flow with temperature differences, heat is lost through radiation at the top of the PV module and into the surrounding environment. Radiative heat transfer and the Stefan-Boltzmann law are temperature-dependent with respect to the temperature difference between the module surface and the outside air. Thermal losses from the bottom surface are like those on the top side, except that this surface is oriented differently relative to the ambient air and the flow. The tilt angle affects forced convection at the bottom, and the heat exchange is computed using a nearly identical formula to that used on the top surface, with some tilt-angle-dependent modifications. Conversely, the inflow angle and its interaction with the bottom surface, modeled after the natural convective coefficient, is described by a correlation similar to that used to define the top surface, but adjusted to the tilt angle. The thermal losses from the bottom surface can be expressed using the same relation given for the top surface [23].

$$Q_{th,\ loss,bottom} = \left(Q_{Forced,\ conv,\ bottom} + Q_{natural,\ conv,\ bottom} + Q_{rad,botoom}\right) \quad (8)$$

For the top and bottom surfaces, mixed convection is employed, involving both forced and natural convection. This is because, in most real-life situations, both processes occur simultaneously. Regarding the Nusselt numbers, the net convective heat transfer coefficient is the sum of the forced- and natural-convection Nusselt numbers. The PV panels have a tilt angle β that influences convective losses and radiative heat transfer. Convective heat transfer is greatly enhanced when the panel is tilted, as this affects the airflow around it. The forced convective coefficient can be estimated from the correlation [23]:

$$h_{F,b} = h_{F,t}\left(\frac{90^{\circ} - \beta}{90^{\circ}}\right) \quad (9)$$

Where $h_{F,t}$ is the convective coefficient at the top surface, and hF,b is the convective coefficient at the bottom surface. The natural convective coefficient can be obtained from the correlation [23]

$$Nu_{N,b} = \frac{h_{N,b}L}{K} = 0.27(Ra_L)^{0.25} \quad \text{If } \beta = 0 \quad (10)$$

$$Nu_{N,b} = 0.7386(Ra_L)^{0.1826}\,(1 + \cos\beta)^{-0.4575} \quad \text{If } 0 < \beta \le 45° \quad (11)$$

$$Nu_{N,b} = 5.4412(Ra_L)^{0.1102}\,(1 + \cos\beta)^{-0.085} \quad \text{If } \beta > 45° \quad (12)$$

Therefore, the mixed convective coefficient is calculated using the formula:

$$Nu_{M,b}^{3} = Nu_{F,b}^{3} + Nu_{N,b}^{3} \quad (13)$$

2.2. The thermal analysis assumptions

It is assumed that all material properties are isotropic and independent of temperature. The reflectivity of the various materials is considered of utmost importance to the analysis. Solar irradiation is not reflected on any surface and is completely passed to the surface beneath. The transmissivity of the EVA is assumed to be one. Internal reflection between the upper EVA and the solar cells is accounted for, but other internal reflections between layers are deemed unimportant. The portion of solar irradiation not reflected by the cell or turned into electricity is transformed into thermal energy. The ambient temperature is uniform across all areas exposed to the environment.

2.3. Simulation assumption

In this study, all material properties used in the photovoltaic (PV) panel model are assumed to be isotropic and temperature-independent, thereby simplifying computation. Broadband optical assumptions from the literature are used instead of idealized values for the EVA encapsulant layer. Notably, EVA transmissivity is assumed to range from 0.85 to 0.90; reflectivity around 0.05 to 0.10, and the remaining fraction consists of absorptivity, as is expected in light of the optical behavior of a solar panel in the solar range (300–1100 nm). These values provide more realistic light transmission and losses through the EVA layer, increasing model fidelity compared to the unrealistic 1.0 and 0.0 reflectivity transmissive values. The solar irradiance reflected from the external layers of the panel, such as ETFE or glass, is assumed to have a standard reflectivity of about 0.07-0.10, which affects the actual energy generation across the Si cells. High silicon cell-layer absorptivity (0.90 to 0.97) and low reflectivity (~0.03) are assumed, consistent with its status as an active photovoltaic material. Internal reflections are simplified between the layers; only the reflection between EVA and solar cells is considered significant. The incident solar radiation is 1000 W/m², and the PV cell can be assumed to act as a heat sink in thermal equilibrium, capable of converting absorbed solar energy into electrical energy. It has been carefully chosen in both the mesh properties and the spatial resolution to achieve a converged model and numerical accuracy. The mean skewness values were below 0.025, and the orthogonal quality was close to unity. A combination of these assumptions will enable simulation of the thermal characteristics and airflow effects on the temperature and power output efficiency of the PV panel at various wind speeds. The values in Table 2 below indicate the values of material (Emissivity(ε)values) applied in the simulation.

Table 2. Emissivity values of photovoltaic panel materials

Material	Emissivity (ε)	Source/Reference
Glass (cover layer)	0.89 – 0.92	[23]
EVA (encapsulant)	0.85 – 0.92	[17]
Silicon (solar cells)	0.75 – 0.85	[19]
Back sheet material	0.85 – 0.95	[22]

These values are an average value of all infrared spectrums of interest at characteristic operating temperatures (~300-400 K). Emissivity depends on surface finish, roughness, and temperature; as mentioned, emissivity is typically measured for PV manufacturing materials. The emissivity is generally high because glass is smooth and polished, and it can effectively radiate heat through its surface (~0.90). EVA encapsulant can exhibit relatively varied values depending on formulation and surface treatment, but typical broadband values are around 0.85–0.90. Silicon solar cells have lower emissivity (~0.75–0.85) according to surface texture and antireflective coating conditions. Back sheets have high emissivity (>0.90) to facilitate thermal radiation.

In performing the numerical simulations in ANSYS Fluent, airflow was modeled as approaching the PV panel, consistent with common engineering work on inclined panels, where ambient airflow is expected to be parallel to the ground and therefore hits the panel at its tilt angle, i.e., oblique to the panel surface.

2.4. Pv model mesh

The quality of the mesh in ANSYS models of solar PV panels is crucial for determining how easily the model can be transported. The measures of mesh integrity typically employed include three met-

rics: skewness, orthogonal quality, and average element quality. The solution's skewness is very high (near 1), which can lead to convergence issues and a numerically unstable heat-transfer simulation. However, the skew toward low value (< 0.5) improves simulation and reliability, as shown in Table 3 below. The closer to 1 quality is an orthogonal quality, which indicates that the elements correspond with the expectation of the solver to which these elements were to be applied, especially in the lay (boundary) resolution in CFD. Any figure less than 0.1 will be considered bad and can bring thermal forecasting to its knees. An average mesh quality, a composite measure of element shape, skewness, and alignment, is recommended, with the average mesh quality held above 0.8 in solar PV panel thermal calculations, where reliable calculation of temperature gradients and uniform heat transfer across panel surfaces is required [23]. Poor accuracy in these quantities may lead to false hot-spot forecasts, resulting in an inadequate assessment of the thermal performance of PV systems. Therefore, ANSYS requires refined meshing and quality checks to model the cooling and heating effects of solar energy modules.

Table 3. Skewness and cell quality [24]

Value of Skewness	Cell Quality
1	degenerate
0.9 — <1	bad (sliver)
0.75 — 0.9	poor
0.5 — 0.75	fair
0.25 — 0.5	good
>0 — 0.25	excellent
0	equilateral

The following paragraph explains the PV panel model's mesh parameters and conditions. The mesh will start with a 10 mm element along all model edges, using a high smoothing option and hard behavior. The multi-Zone mesh method with a Hexa-mapped, uniform surface mesh is used for the Si cell layer. The mesh was also chosen as a Hexa type with free mesh and linear elements to ensure the best element order and distribution for each Si cell, as shown in Figure 2 below. The choice of element size starts from 10 mm. The mesh quality is checked for skewness and orthogonal conditions. The best element size should have an average skewness value between 0 and 0.25, with an orthogonal quality value between 0 and 1, where 0 is the worst, and 1 is the best. According to these conditions and the results in Table 4 below, the 7 mm element size was the suitable choice for this simulation model's meshing, yielding the best orthogonal average value just below the single value.

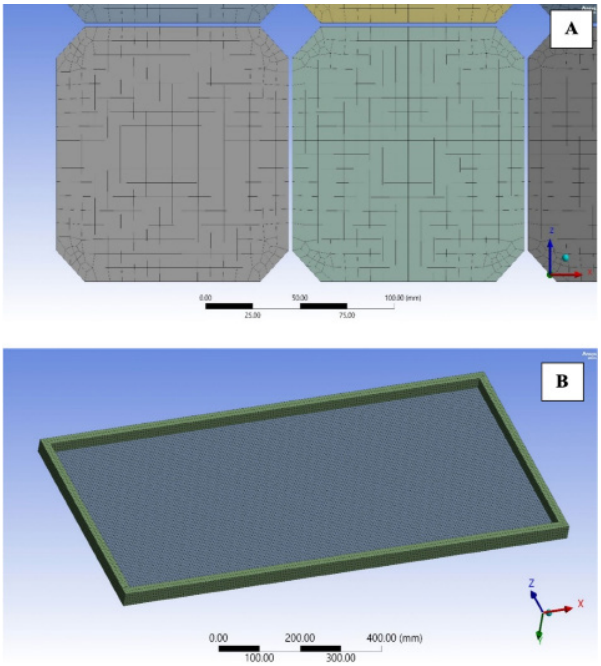

Figure 2. (A) PV panel Si cells mesh, and (B)the model multizone mesh method arrangement

Table 4. Mesh parameters according to the element size

Element size	Elements No.	Nodes No.	Skewness average	Orthogonal average
10 mm	45568	291482	1.63e -002	1.1364
9 mm	54968	355864	1.80e -002	1.0961
8 mm	69989	452563	1.74e -002	1.0141
7 mm	90728	578782	1.24e -002	0.9964
6 mm	127890	808060	1.15e -002	0.9136

2.5. Integration of mesh quality and thermal model

Mesh generation is not a separate step in computational thermal modeling of PV panels; rather, it is a fundamental part of accurate heat transfer modeling. The accuracy of the temperature profiles obtained on a spatial scale and the heat flux calculated using ANSYS-based simulations is sensitive to mesh quality metrics such as skewness, orthogonal quality, and average element quality. Numerical instabilities arise from poor mesh quality, especially in thin boundary layers, where steep temperature gradients set the threshold for the efficiency of both forced and mixed convection. For instance, simulations with high skewness or low orthogonality can distort the thermal boundary layer thickness and the heat-dissipation rate of Si cells. Here, mesh parameters were selected to match physical behavior in the mixed- and forced-convection ranges. A multi-Zone mesh with Hexahedral elements, with a mean skewness below 0.15 and orthogonality near 1, allowed the mesh to accommodate the relevant boundary layer near the PV panel, where the

maximum temperature decreases occurred. Thus, the mesh convergence study concluded that decreasing the element size from 10 mm to 7 mm improved the accuracy of local heat flux forecasting and strengthened the correlation between wind speed and cell temperature, confirming that the mesh quality could effectively capture all differences. For instance, the thermal gradients captured in the 7 mm mesh align directly with the numerical performance of the reference experimental results, demonstrating the mesh's ability to capture the airflow's true dependence on thermal dissipation.

2.6 Boundary conditions and mesh-thermal

Boundary conditions such as stipulated heat fluxes, convective coefficients, and set or ambient-temperature surfaces are physically meaningful only if the mesh supports a stable, accurate solution of the governing equations. Heat conduction in the panel layers and convection at the panel-solid interface were also modeled in the simulation using properly chosen mesh element sizes and high-quality cell metrics. The fact that the simulated cell of the Si minimized uncertainty in temperature and that the numerical artifact (e.g., globally infamous hot spots) is also evidence of the positive relation between mesh quality and thermal results. The mesh quality and refinement will provide reasonable estimates of cooling efficiency, thermal stress, and the risk of long-term degradation of PV modules under different wind conditions. Thus, the meshing and choice of boundary conditions can now be better justified and aligned with the predictive ability of the thermal model, thereby enhancing the trustworthiness of both the scientific results and those made by the engineer.

2.7. Heat flux calculations and the boundary conditions

The boundary conditions of this simulation are based on real PV panel specifications to achieve more realistic results and maximize their relevance to real-life applications. The PV panel's Si cells produced 70 W at a working temperature of 25 °C and an incident solar radiation (q solar) of 1000 W/m^2. The optical properties of PV panel layers are defined by three parameters, i.e., absorptivity (α), transmissive (τ), and reflectivity (ρ), fulfilling the energy conservation equation as follows:

$$\alpha + \tau + \rho = 1 \quad (14)$$

Each term represents the fraction of incident solar irradiance absorbed, transmitted, or reflected by the material, respectively. It should be noted that reflectivity (ρ) is the fraction of radiation reflected away from the surface and not absorbed or transmitted through the layer. A reflectivity value of 0.10 means that only 10% of the solar irradiance is reflected, not absorbed. Then the remaining percentage (derived from transmissivity and reflectivity, respectively) gives the absorbed energy fraction. Accurate interpretation of optical parameters is needed to determine the optimal energy balance across the panel layers, temperature distributions, and actual performance. Table 5 summarizes the transmissivity and reflectivity values for each layer, using established optical properties literature to reflect the transmissivity and reflectivity available in the public domain, thereby enabling physically consistent simulations. The sequence of PV panel layers is illustrated in Figure 3, and their absorptivity, transmissivity, and reflectivity are listed in Table 5.

Table 5. The physical properties of the first three layers.

Material	Absorptivity	Transmissivity	Reflectivity
ETFE	0.1	0.83	0.07
EVA	0.0	1.0	0.0
Si	0.97	0.0	0.03

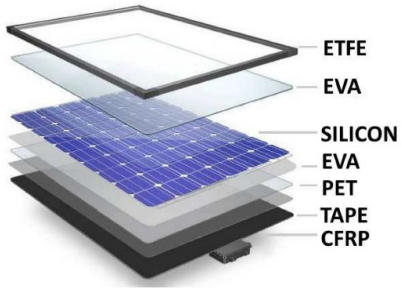

Figure 3. PV Panel Layers Sequence Layout [26]

According to Figure 3, the first three layers were the ETFE, then EVA, and the last layer was silicon cells. According to Table 4, the ETFE Absorptivity was 0.1 for 1000 W/m2 incident solar radiation (q solar), corresponding to 100 W/m2, and 0.07 was reflected, resulting in 70 W/m2 in optical losses. The 100 W/m^2 will be set as the ETFE layer heat flux value; the second EVA layer has zero absorptivity and reflectivity, and the heat flux for this layer will be produced from the silicon cell layer. The incident solar radiation from the first layer has a transmissivity of 0.83, corresponding to 830 W/m2, and will transfer to the third silicon cell layer. This layer has a reflectivity of 0.03, which means 0.03 of the 830 W/m2 will be reflected to the second layer above it, so the heat flux for the second layer will be 24.9 W/m^2.

The heat flux for the third layer will equal the transmitted incident solar radiation from the first layer (830 W/m^2) minus the reflected heat flux (approximately 25 W/m^2), which equals 805 W/m^2. As mentioned above, the third silicon cell layer also generates a heat flux at its surface, arising from the PV panel's power output (70 W). To transform this value to heat flux, the generated power must be divided by the total surface area of the 36 Si cells in this layer. In the ANSYS modeler, the single cell surface area is 0.01468 m2; for 36 cells, it is 0.52848 m^2. So, the surface heat flux will be 70 divided by 0.52848, which equals 132.455, and the total heat flux for the third layer will be 805 minus 132.455, which equals 672.455 W/m^2. The first and last layers (ETFE and CFRP) will experience heat radiation, and they must be treated as boundary conditions using the emissivity value (0.89) from Table 4 above for both layers. The Si

layer in the PV panel absorbs some of the energy from incident solar radiation and transforms part of it into electrical energy. The rest is absorbed as heat. The electrical power generated corresponds to the energy removed and is therefore considered a heat sink (i.e., energy removed) for the Si layer in the thermal model. The optical losses in the outer layers (e.g., ETFE and EVA) reduce the amount of solar radiation reaching the Si layer. For example, with incident radiation of 1000 W/m², after losses in the previous layers, only around 830 W/m² reaches the Si layer. The heat flux absorbed by the Si layer is calculated by subtracting the reflected portion at the Si surface from the transmitted radiation. In this example, approximately 805 W/m² reaches the Si layer after reflection losses. The electrical power generated by the PV cells, for example, 70 W total across 36 cells, is energy diverted from heat storage and does not contribute to temperature rise. This power is treated as a heat sink by converting it into a heat flux value after dividing the total generated power by the total Si cell area (surface area). For 36 cells with a total area of 0.52848 m², the power-generated heat flux is 70 / 0.52848 ≈ 132.455 W/m^2. The heat flux that decreases the electrical power absorbed (heat sink) is the net heat flux absorbed (changed to heat) by the Si layer:

Q net = Q absorbed – Q generated power, using the example numbers:

$$805W/m^2 - 132.455W/m^2 = 672.545W/m^2$$

This net flux is the heat load that drives the rise in temperature of the Si layer. In electrical generation, a heat sink is designed to reflect the physical reality that it essentially absorbs energy in the thermal system, thereby reducing the heat load on the object's total radiation. This matches optical and electrical energy flows, enabling the thermal simulation to predict the real cell temperature of Si under operating conditions. Adding this heat sink term to the energy balance and boundary conditions of the Si layer can enable the model to capture the interactions between electrical output and thermal behavior, as observed with increased airflow (greater convection), which reduces silicon cell temperatures and thereby increases power efficiency. The computational domain may include the PV panel and a sufficient surrounding air region to prevent boundary effects (blockage ratio <5% relative to the inlet cross-sectional area, based on a preliminary domain sensitivity test). Dynamic equilibrium temperature modeling and controlled airflow modeling representing normal operating conditions were used to perform steady-state simulations. Effects of turbulence are modeled using the k–ω SST turbulence model, which provides superior treatment of wall structures, with y+ values between 1 and 3 to resolve the boundary layer. Radiative heat transfer was modeled using the Discrete Ordinates (DO)radiation model, if the media (air with negligible absorption/scattering) was excluded. The thermal contact resistance between the PV layers were neglected due to their negligible thickness, which also meant good thermal contact within the normal construction of a PV panel. These boundary conditions include a velocity inlet and a pressure outlet for airflow, symmetry conditions at the lateral domain boundaries, and convective and radiative heat exchange across exposed surfaces. Second-order terms in the momentum, energy, and turbulence equations were used for numerical accuracy in the spatial discretization. Residuals were set to 10–6 for all transport equations, and stability was ensured by monitoring key solution variables, such as the maximum silicon cell temperature and other parameters. The convective heat transfer between the upper and lower layers will be calculated using the following equation. [25]:

$$h = \frac{N_u \times k}{L} \quad (15)$$

Where: Nu is Nusselt number, k is the thermal conductivity of air (approximately 0.0257 W/m.K at room temperature), and L is the characteristic length of the surface. The Nusselt number can be calculated from the following equation:

$$Nu = C \times Re^m \times Pr^n \quad (16)$$

Where: Cm, and n are constants that depend on the geometry and flow conditions. For forced convection over a flat surface, typical values are: $C = 0.332$, $m = 0.5$, and $n = 0.33$. (Pr) is the Prandtl number, which equals 0.6904, and Re is the Reynolds number, which is calculated from the following equation [26]:

$$Re = \frac{U \times L}{V} \quad (17)$$

Where: U is the wind velocity (4 m/s), L is the characteristic length of the surface, and ν is the kinematic viscosity of air (m²/s), which is temperature dependent. From the above equations, the wind speed variation will change the value of the mixed convection coefficient (h) in equation (13) and, in turn, the Si cells' temperature and the generated power. Figure 4 below illustrates the effects of mixed convection and its direction on the PV panel.

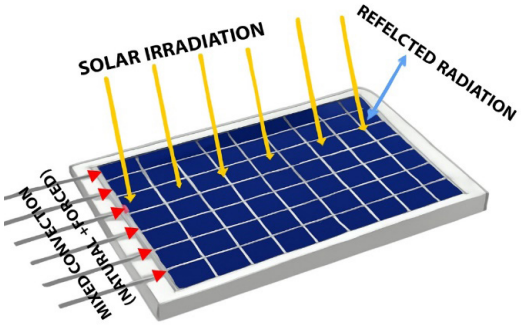

Figure 4. The PV panel mixed convection, solar irradiation, and reflected radiation direction

The numerical simulation carried out in this study is a three-dimensional (3D) steady-state thermal analysis using the software ANSYS Fluent to represent the actual spatial temperature distribution and

airflow on the PV panel. The PV panel modeled for simulation is a traditional monocrystalline silicon module with 36 cells in a six-by-six configuration. The surface area of each Si cell is equal to ~0.01468 m^2, and the Si cell layer area is equal to ~0.52848 m^2. The 36-cell combined size (the total panel size) is proportional to the size of an average panel, the average surface area is 0.52848 m2, the active surface length (parallel with the wind flow) is approximately 0.3 m, and a width that differs with the number of cells (that of a commercial panel is typically comparable). The mesh construction is performed using a multi-zone approach with hexahedral (Hexa) elements to achieve a structured, uniform cell field, particularly in the Si cell layer and the boundary layer. In a mesh convergence study, the element dimensions ranged from 6 mm to 10 mm. The choice of an optimal element size of 7 mm is the preferred minimum size to achieve the highest resolution and optimal solution accuracy at the lowest computational cost. Mesh spatial resolution is chosen to ensure that the thermal boundary layer, which has steep temperature gradients, is resolved; mesh resolution is directly controlled. This made it possible to perform effective computations of the convective heat transfer coefficient and the panel's surface temperature distribution. All skewness values for the average mesh were less than -0.25, and the orthogonal quality approached the skewness level that meets ANSYS CFD criteria, indicating good mesh and numerical quality. This 3D mesh resolution and model dimensioning allow the forced versus mixed convection regime, temperature gradient of the Si cells, and overall thermal characteristic of the PV panel to be captured with high accuracy.

2.8. Optical-thermal energy budget per layer

In these simulations, the authors assume the total solar irradiance incident on the PV panel surface is 1000 W/m^2. Layer-wise Optical Budget (Incident → Reflected → Transmitted → Absorbed). The energy flows are computed for each layer (ETFE, EVA, Si cell). For the ETFE Layer, the Reflectivity (ρ_{ETFE}) ≈ is 0.07, so 7% of the incident radiation is reflected (optical loss). Transmissivity (τ_{ETFE}) ≈ 0.83, allowing 83% of the signal to be transmitted to the next layer. Absorptivity (α_{ETFE}) = 1 − ρ_{ETFE} − τ_{ETFE} = 0.1, reflecting the absorbed energy transformed into thermal energy in ETFE. The transmissivity (τ_{EVA}) for the EVA Layer is 0.85–0.90(realistic assumption). Absorptivity (α_{EVA}) and reflectivity (ρ_{EVA}) sum to the remaining fraction, with reflectivity typically low. The absorbed energy in EVA raises its temperature. The low reflectivity (ρSi) ≈ is 0.03 for the Silicon Cell Layer. Absorptivity (α_{Si}) is high (~0.90), so most transmitted energy is absorbed. Silicon cells absorb energy as heat, which generates heat and electrical energy. Electrical power generated, $P_{elec,}$ is calculated as:

$$Pelec = \eta \times G \times A$$

where η = efficiency (either experimental or literature), G = incident irradiance, and A = total Si cell surface area. As electrical generation removes energy from the system, this power acts as a heat sink (energy removed) in the Si cell energy balance, reducing thermal heat generation. In the Si layer, the net heat generation is then: $Q_{net} = Q_{absorbed} - A_{Pelec,}$ where $Q_{absorbed}$ is the absorbed solar radiation heat flux. The removal of electrical power is used as a heat-flux boundary condition (sink) on the Si cell surface, thereby reducing the source term of the heat-flux field. This converter converts solar energy into useful electrical energy, minimizing heat production and, therefore, panel temperature.

3. Results and discussions

The following figures and table illustrate the effects of inlet air velocity at a typical ambient temperature of 25 °C on the Si cells' temperature. Starting from an air velocity of 1 m/s, the mixed convection in the Si cell layer is calculated, and ANSYS is used to show the temperature and thermal distribution. This procedure is repeated for air velocities of 2, 3, 4, and 5. Figure 5 (A) and (B) below illustrate the maximum and minimum temperature and the thermal distribution at the Si cells layer and the PV panel.

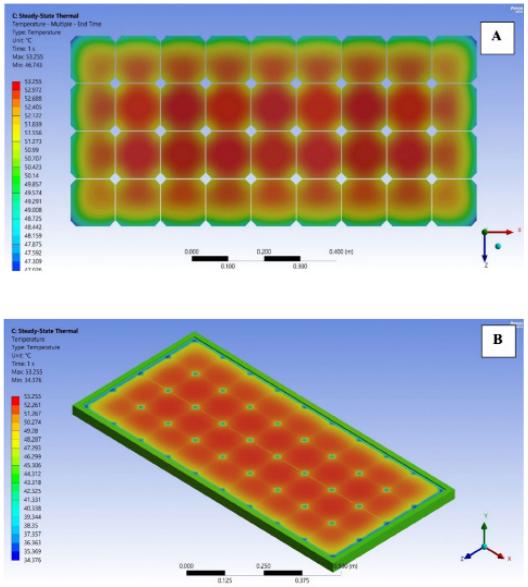

Figure 5. Maximum and minimum temperature and thermal distributions for 1 m/s inlet velocity(A)Si cells layers, and(B)PV panel

Figure 5 (A) and (B) show the temperature distributions at a silicon cell layer in a photovoltaic (PV) panel and the whole PV module, respectively. The temperature readings are also significant in both pictures: the highest is around 53.255 °C in Figure 5 (A) and 34.376 °C in Figure 6 (B), and the lowest is 46.743 °C in Figure 5 (A). These variations indicate how much thermal energy is radiated across the module's entire surface. The differences in Figure 6 (A) are a product of thermal absorption in the silicon (Si) cells, the active material that makes up the device, subsequently heating the localized areas. The transmission of this temperature increase occurs through heat conduction and convection, producing temperature gradients of 46.75 °C to 53.3 °C, likely due to differences in thermal conductivity and the convective atmosphere around the panel. Figure 5 (B) shows the

complete temperature profile of the module; the module temperature is highest in the hot region (33.255 °C) and decreases to 34.376 °C at the cold junction. The least directionally exposed regions of solar irradiance, or those regions of an air mass with paved areas or external surfaces of surface-cooling material, are the low-temperature spheres (less than 34.376 °C), which are statistically the least accessible. [27].

The simulation results show that the heat loss rate of photovoltaic (PV) panels depends on the inlet air speed, which is the most important parameter. The present analysis shows a constant inlet velocity of 1 m/s. At such a velocity, mixed-mode convective heat transfer, also known as mixed convection, appears in the system. In mixed convection, natural convection driven by spontaneous density currents due to the temperature gradient occurs simultaneously with forced convection due to air movement. The greater the air velocity, the more pronounced the forced-convection effects, thereby increasing the heat-removal performance of the PV surfaces. However, at low velocities, such as 1 m/s, forced convection is only relatively inefficient compared to velocities above 3 m/s. In these circumstances, the passing air creates a boundary layer on the surface of a PV module, generating a high-temperature contrast. Low-velocity boundary layers are intense and resistive, thereby impeding heat dissipation. On the other hand, layer thickness in the boundary layer decreases at higher velocities, the gradients become smaller, and the convective heat transfer rate increases. As such, the thermal resistance of the air layer decreases, resulting in greater cooling. When the inlet flow is reduced to 1 m/s, the convective heat transfer rate decreases, and hence the module temperatures increase, as indicated in the simulation data plot, peaking at 53.255 °C.

For photovoltaic (PV) modules, it is necessary to determine the spatial radiation distribution (in terms of the silicon (Si) layer) using the air velocity. Experimental studies show that the convective heat-transfer coefficient increases with air velocity, thereby decreasing the temperature of the surface layer. Although the available power of the machine to increase heat extraction has been moderately boosted at a velocity of 1 m/s, the best performance is observed at higher velocities, i.e., 3-5 m/s. What is important here is that, with the Si layers hot, the recombination rates must be high, which will consequently lower the open-circuit voltage and the overall efficiency of the module. The extended stay under high temperatures also results in thermal expansion and, correspondingly, mechanical stress, which can compromise material integrity. [28]. The overall temperature distribution within the panel is therefore representative of the Si-layer's overall effects and the cooling mechanism, which is by air flowing at 1 m/s. Thermal non-homogeneity occurs naturally: areas where airflow is stronger cool faster, and regions in the center experience more intense heat buildup due to low convective capacity. Effective heat dissipation is critical to proper thermal balance in the module and, consequently, to its operational functionality. When air velocity equals the ventilator's movement, the system is thermally disadvantaged at 1 m/s.

Figures 6 (A) and (B) illustrate the Si layer, PV panel temperature, and thermal distributions. Figure 6(A)shows that the maximum temperature inside the silicon cell layer increases to 47.011 °C and the minimum decreases to 41.376 °C, at a wind speed of 2 m/s. Figure 6(B) shows the matching panel temperature distributions, yielding a maximum value of 47.011 °C. Minimal value of 30.884 °C. Such values indicate that, compared to the 1 m/s conditions, under which the highest temperatures at the cell layers were found to be 53.255 °C, the increased air velocity has reduced both the extreme and mean cell-layer temperatures by ~6.2 °C. The matching minimum temperature also drops similarly by 46.743 °C to 41.376 °C upon the imposition of 2 m/s. Notably, the heat flux distribution over the silicon cell layer is relatively uniform at higher velocities, implying more even convection and heat transfer through the boundary layer, resulting in more uniform heat removal. The spatial profile indicates that the gradient is smoother, and the center point of the profile barely suggests it is hotter than the outer regions.

A similar pattern is observed in the total number of PV panels in the 2 m/s case presented in Figure 6 (B): the maximum temperature is 47.011 °C, and the minimum is 30.884 °C. This significantly improved the 1 m/s case, where the minimum temperature was approximately 34.376 °C. The enhanced convective heat transfer rates at high velocity are evident in the temperature profiles shown in Figure 6 (B), where cold water has colonized a significant portion of the PV surface by many degrees. At 1 m/s, the dominant heat-removal process is mixed convection, which, in this instance, is primarily natural convection since the air flow is rather small [29].

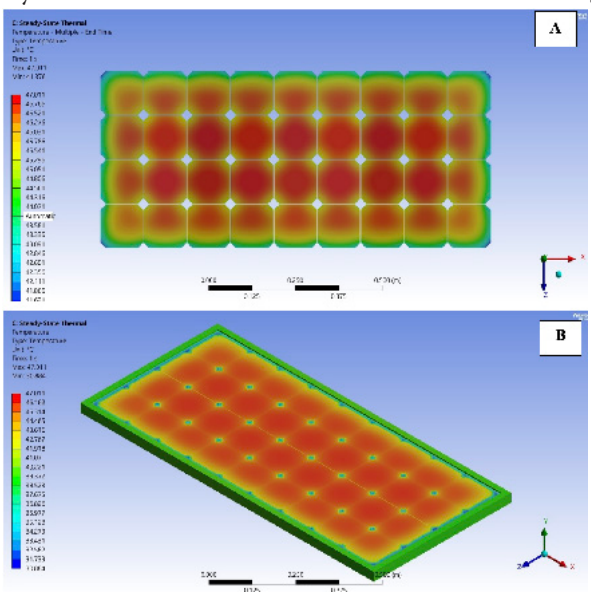

Figure 6. Maximum and minimum temperature and thermal distributions for 2 m/s inlet velocity(A)Si cells layers, and(B)PV panel

The comparatively slow flow leads to a thicker thermal boundary layer near the surface, reducing heat dissipation capability. At an air velocity of 2 m/s, forced convection is more dominant; the air's ki-

netic energy helps reduce the thermal boundary layer and optimize heat removal from the Si cells and the entire PV module. The role of forced convection thus increases the overall heat-transfer rate.

Since the flow velocity is low at 1 m/s, efficiency is low due to a thicker boundary layer, leading to high temperatures and a high thermal gradient throughout the Si-cell array. Only the boundary layer reduces at 2 m/s; therefore, with more vigorous mixing of ambient air with near-surface air, heat exchange increases, and temperature changes are smoothed. At 1 m/s, the maximum temperature in the Si-cell layer is 53.255 °C, indicating low heat-removal efficiency at this velocity, leading to non-uniform cooling. In comparison, at 2 m/s, a maximum layer temperature of 47.011 °C is attained, a decrease of about 6.2 °C, which translates into efficiency advantages elsewhere demonstrated by eliminating the detrimental thermal effects. PV-panel temperatures correspondingly show relevant differences. The maximum temperature of the panel reaches 53.255 0 C at a velocity of 1 m/s, which is conducive to greater rates of efficiency deterioration and a higher probability of thermal deterioration, particularly in high-performance modules. Conversely, PV operating temperature at the upper 2 m/s, minimizing overall heat-related losses and the resulting strain on the system, and perhaps extending parts' lifespans. Generally, higher temperature loads compromise the working temperature, effectiveness, and long-term stability of the PV cell at flow velocities below 1 m/s. Raising the airspeed to 2 m/s enhances cooling, enables operation of Si-cells to achieve a greater effect, and consequently improves overall system performance, mitigating thermal fatigue and extending PV-panel lifespan. [30].

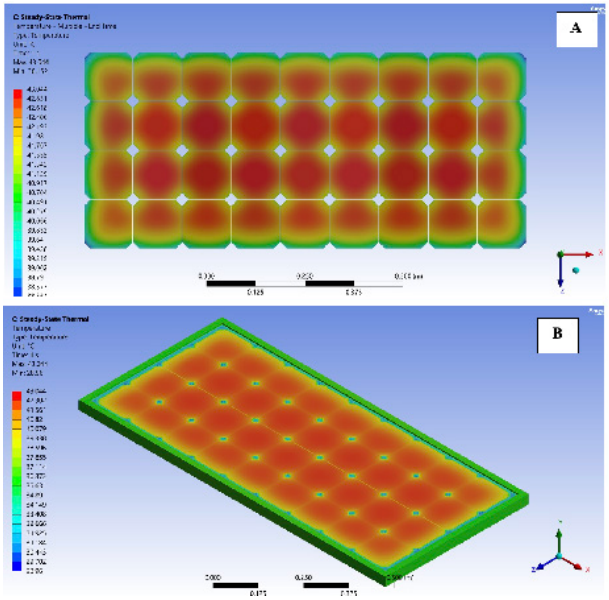

Figure 7. Maximum and minimum temperature and thermal distributions for 3 m/s inlet velocity (A) Si cells layers, and (B) PV panel

Figure 8(A)and(B)illustrate the Si layer and PV panel temperature and thermal distributions of 3 m/s air velocity. Having realized the layer velocities of 3 m/s, the thermal gradients are significantly narrower than at 1 m/s or 2 m/s. Under the Si cell layer in Figure 8 (A), the reported maximum temperature falls to 43.044 °C, 10.2 °C lower than that at 1 m/s (53.255 °C) and 4 °C lower than that at 2 m/s (47.011 °C). Minimum temperatures decrease as well: 38.152 °C in Figure 8 (A) compared with 39.003 °C at 1 m/s and 41.814 °C at 2 m/s. Such observations show that the higher velocity is more efficient in cooling. The results in Figure 8 (B) show that the highest temperature of the PV panel was 43.044 °C, which is 10.2 °C lower than at 1 m/s and 4 °C lower than at 2 m/s, resulting in the lowest temperature of 28.96 °C. These results identify the increased heat dissipation with increased velocities. At 3 m/s, the primary mode of heat transfer is forced convection, as evidenced by a reduction in thermal boundary layers. A reduced boundary layer thickness enables better mixing of the cold air outside the boundary layer with the hot air near the surface, thereby increasing the heat transfer rate. There is less chance of hypostagnant air forming; thus, the total module temperature is lowered. The thermal boundary layer at 3 m/s is even more dissipated than the 1 m/s and 2 m/s. This effect causes the rapid replacement of air in the surface region by a cooler external stream, smoothing the surface-layer temperature distribution and enhancing heat transfer. At a wind speed of 1 m/s, high ambient temperatures increase thermal losses, thereby reducing the electrical output of the photovoltaic (PV) module. At the same time, the likelihood of thermal degradation in the materials increases, thereby reducing the overall life expectancy of the PV system. A higher wind speed of 2 m/s provides more effective cooling, resulting in a lower Si-cell temperature and increased electrical efficiency. The peak temperature is reduced by 6.2 °C relative to that recorded at 1 m/s, and the direct effect is an extended operational longevity. This results in optimal cooling conditions, achieved at 3 m/s; temperatures in all Si cells and throughout the PV panel are at their lowest, thereby improving efficiency by limiting thermal losses. The temperature reductions of 10.2 °C at 1 m/s and 4.1 °C at 2 m/s will ultimately extend system life by increasing conversion efficiency and reducing thermal strain [31].

Figure 9 (A) and (B) illustrate the Si layer and PV panel temperature and thermal distributions of 4 m/s air velocity. In the case of a PV system that we are investigating it can be seen that there is a clear pattern in the patterns of temperature distributions observed at a variety of wind velocities. With an air velocity of 4 m/s, the peak temperature of the Si cell layer is 40.552 °C, a significantly lower value relative to that at 3 m/s (43.044 °C), 2 m/s (47.011 °C), and 1 m/s (53.255 °C). The 2.5 °C difference between 4 m/s and 3 m/s represents the largest that exists between any pair of velocities. Further, the lowest temperature at 4 m/s(36.163 °C) is significantly lower when compared with the temperatures at 3 m/s (38.152 °C), 2 m/s(41.376 °C), and 1 m/s (46.743 °C), indicating that the higher the air velocity, the higher the thermal gradients and the more homogeneous thermal distribution. Similar remarks can be made regarding the temperatures of the complete PV panel. The panel temperature

at peak is 40.552 °C (reduced by 2.5 °C at 3 m/s and by an order of magnitude more than at 1 m/s and 2 m/s). The corresponding minimum temperature of 27.893 °C cuts even deeper, nearly 3 °C below the 3 m/s temperature and well below any of the other temperatures at which these lows occur. The gradual decline in the overall panel maximum and minimum temperatures corresponds to a significant rise in cooling efficiency.

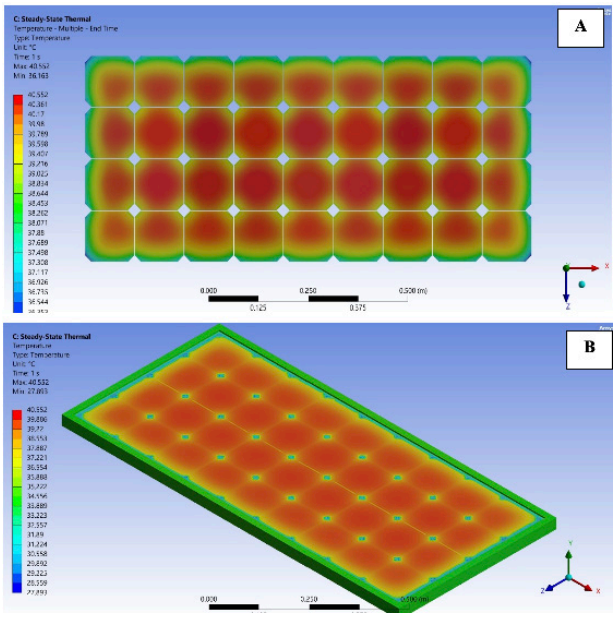

Figure 9. Maximum and minimum temperature and thermal distributions for 4 m/s inlet velocity (A) Si cells layers, and (B) PV panel

As the air velocity increases to 4 m/s, the total cooling efficiency rises considerably, and forced convection becomes the dominant cooling mechanism. Convective mixing remains predominant in this regime, but natural convection plays an essential role because the thick boundary layer slows heat dissipation. Comparatively, forced convection at 2 m/s is increasingly dominant, leading to an increase in the heat transfer coefficient and in bodies with narrow boundary layers. More efficient cooling capacity (as seen at 3 m/s) can also be observed, as the boundary layers formed are thicker; in this case, there should be more mixing of air with the surface, leading to cooler temperatures. At a velocity of 4 m/s, forced convection is complete, the boundary layer is almost negligible, and the surface minimum and maximum temperatures decrease substantially.

The increase in cooling efficiency with increasing flow velocity is accompanied by a corresponding thinning of the bounding layer as flow velocity decreases from 1 m/s to 4 m/s, allowing a more rapid heat exchange with the moving air. The low surface temperatures measured under the minimum boundary layer precipitate have been maximized at the lowest surface temperatures and, correspondingly, have the greatest cooling performance at the highest velocities under examination. At high ambient temperatures and 1 m/s, the system experiences high thermal losses, reduces Si cell efficiency, and increased risk of thermal degradation over long periods of operation. This results in it operating the system below optimal, negatively affecting performance. This can significantly enhance convective heat transfer such that the maximum cell temperature decreases by 6.2 °C at 2 m/s. Performance is reduced slightly, and thermal stress is consequently alleviated. Under these circumstances, the PV module has a longer operating life than when working at 1 m/s. Further increase in the wind velocity to 3 m/s will reduce the maximum temperature by 4 °C compared to 2 m/s and improve system performance. The resulting heat-exchange process is forced convection at this air speed, which enhances both efficiency and durability. The peak cooling is attained at 4 m/s. A maximum cell temperature of 40.552 °C indicates a benign temperature for the Si cells and the entire PV array. System efficiency is optimized, thermal degradation is minimized, and the system sustains the longest operating life and optimal performance. [32].

When the wind is at 5 m/s, the highest temperature found in the Si cell layer in Figure 10 (A) is 38.809 °C, which decreases by 1.7 °C compared to the corresponding level at 4 m/s and 2.0 °C compared to 3 m/s. This observation indicates that the heat-rejection performance of the photovoltaic array improves with increasing wind speed. Comparatively, the lowest temperature in the cell layer is 34.791 °C, thereby defining the amplified cooling effect at 5 m/s. The maximum and minimum temperature differences have decreased, suggesting better spatial thermal homogeneity within the Si cell layer.

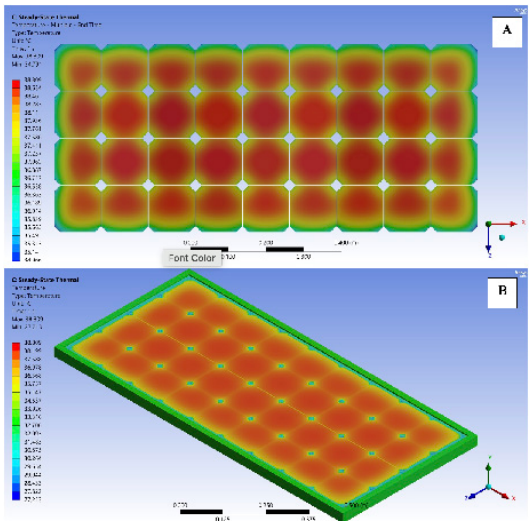

Figure 10. Maximum and minimum temperature and thermal distributions for 5 m/s inlet velocity (A) Si cells layers, and (B) PV panel

Across the entire PV panel shown in Figure 10 (B), the highest temperature is again 38.809 °C, 1.7 °C lower than at 4 m/s and 4.2 °C lower than at 3 m/s. The lowest temperature value of 27.213 °C represents an unprecedented decrease in absolute temperature relative to the earlier velocities and, significantly, a drop of 5 °C relative to

the 1 m/s velocity (32.213 °C) and 1 °C relative to the 2 m/s velocity (28.290 °C). Maximum forced convection is achieved at a wind speed of 5 m/s, significantly enhancing heat dissipation from the silicon (Si) solar cells and the entire photovoltaic (PV) panel. When the heat transfer mechanism changes to mixed convection at 1 m/s, natural convection still plays a significant role in maintaining relatively high surface temperatures, thereby reducing the efficacy of thermal control. At velocities of 2 m/s -4 m/s, the natural convection is progressively replaced by the forced convection, as the physical process cools down and the thickness of the boundary layers reduces. Since the flow has a velocity of 5 m/s, forced convection plays a significant role, and the resulting thin thermal boundary layer most effectively extracts heat from the PV surface. The conditions affected lead to low temperature profiles in both the Si cells and the PV panel, as the fast-moving air aids cooling. [33].

As wind velocity increases, the thermal boundary layer thins, increasing heat transfer between the PV surface and the air near the surface. This is because the cold surface layer is replaced with fresh air as soon as possible to prevent heat from stagnating in the system, and hence the system temperature remains low. Based on empirical experiments, as wind speed increases (1 m/s), the temperature of the Si cells rises, causing thermal stress and leading to lower efficiency and accelerated long-term degradation. Achieving that by a high speed of the wind to 2 m/s will decrease the maximum cell temperature and minimize the risks of thermal degradation and thus will raise operating efficiency. The greater the temperature rises to reach 3 m/s, the greater the airflow cools, which means the Si cells can be operated at lower temperatures, leading to increased electrical performance and elimination of thermal stress. It is kept at a low temperature (4 m/s), and the panel is subjected to the best thermal conditions it has experienced to date, thereby optimizing efficiency. The panel's lifespan is extended even further. Finally, a wind speed of 5 m/s offers the greatest cooling ability and yields the lowest temperatures across the entire device, which can enable the Si cells and the PV module to operate at peak efficiency with minimal thermal degradation and optimal reliability. Table 6 below will compare five velocities of air (1, 2, 3, 4, and 5 m/s) and the temperature of the active layer of the PV panel (Max and Min) to illustrate how the active layer of the PV panel heats under different cooling conditions, 53.255 i C in the Si cells at 1 m/s but 38.809 °C in the Si. The overall thermal load of the glass and frame is reported by the PV Panel Temperatures (Max & Min).

Table 6. Comparison of the Si cells and PV panel temperature at different air velocities.

Air Velocity (m/s)	Si Cell		PV Panel		Impact on Power & Convection
	Max Temp (°C)	Min Temp (°C)	Max Temp (°C)	Min Temp (°C)	
1	53.255	46.743	53.255	36.163	High temperatures, mixed-convection-dominated, thick boundary layer, low power output, high thermal stress.
2	47.011	41.376	47.011	34.376	Temperature reduction ~6.2°C; forced convection is more effective; improved cooling; increased power; reduced thermal stress.
3	43.044	38.152	43.044	28.960	Further temperature drops of 4°C; forced convection dominant; thinner boundary layer; better cooling; higher power output.
4	40.552	36.163	40.552	27.893	Maximum temperature reduction 2.5°C; forced convection fully established; uniform cooling; optimal efficiency; minimal thermal stress.
5	38.809	34.791	38.809	27.213	Lowest temperatures; forced convection maximized; thermal boundary layer nearly eliminated; optimal power output; minimal degradation.

This evidence shows that increased airflow has a cooling effect on the cells and the panel as a whole and appears to be the key to improved structural stability and reduced stress. In addition, the findings explain the effects on Mixed Convection and Power Generation and show that air velocity is the primary determining factor for the dominant heat-transfer mechanism. Mixed convection is dominated by Natural convection, thick boundary layers, and inefficient cooling at low speeds (1 m/s to 2 m/s). On the other hand, at large velocities (3 to 5 m/s), it becomes apparent that forced convection is predominant, the boundary layer is thin, and heat is more easily removed. High temperatures, as indicated in the sequences, will reduce electrical output due to lower open-circuit voltage. In contrast, effective cooling will improve production, reduce thermal degradation, and extend life. Such findings have an obvious physical interpretation: the higher the air velocity, the greater the component of forced convection in mixed convection [34]. Increasing the air velocity over the PV panel from 1 m/s to 5 m/s systematically reduced the maximum and minimum temperatures of the silicon layer and the entire PV panel. The observed drop was largest at 1-2 m/s and decreased (but only positively) with increasing airflow. Overall performance

showed about a 14.5°C reduction in silicon cell temperature between 1 m/s and 5 m/s (around 53.3°C at 1 m/s with mostly mixed convection and a thick boundary layer, or 38.8°C at 5 m/s with dominant forced convection and a thin boundary layer). Low-to-moderate velocity results in a quick downward tendency. When further increase in m/s, the rate of performance decreases to approximately 3 m/s, and the air temperature approaches an asymptote, where performance rates are very high. The maximum PV panel temperature decreased by the same percentage, indicating good heat loss in the panels with or without wind. The mixed convection at low velocities (12 m/s) is indeed dominated by natural convection, and the cooling effectiveness is in a less favorable position than usual. The limit for forced convection is above 3 m/s (higher temperatures in general, better cooling, improved performance). The low panel temperature achieved with high air velocities has been shown to improve electrical efficiency and minimize thermal stress, material degradation, and hotspots. The cooling efficiencies can contribute to both short-term and long-term power generation of the PV system and system durability.

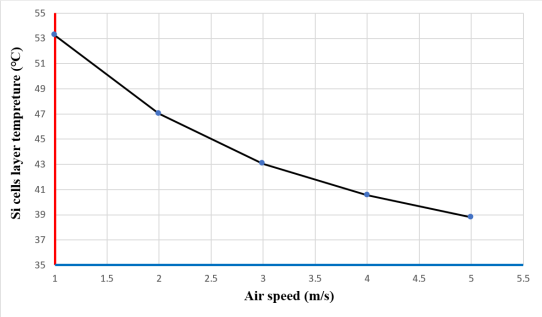

Figure 11. Chart of air speed (m/s) vs. temperature of the Si cell layer

The findings of the ANSYS model, as shown in Fig. 11, can then be interpreted freely considering a physical-intuition viewpoint. The forced-convection component of mixed-convection heat transfer is assuming an increasingly larger role as air velocity increases. This strength effect reduces the thickness of the thermal boundary layer on the PV array surface, allowing it to dissipate heat more easily. It means that the highest point of the front side temperature of the solar cells is. Max) and lowest (Temp.). The minimum temperatures will be lowered, which implies reduced thermal stress on the silicon monocrystalline cells. The distribution of cooling across the panel and the temperature were caused by no longer clumping at the edges. Min drop is astounding. As the data also show, there is some nonlinearity in the response: the largest decrease in temperature. Maximum speeds of 1 and 2 m /s; then the rise in velocity thereafter is comparably smaller with considerably less improvement at the former, which tends towards an asymptotic decrease in Temperature. This upper limit is as close to the minimal possible as possible. The response of a PV cell has been known to be affected by temperature; the higher the cell temperature, the lower the value of open circuit voltage (Voc) and the system's overall generation. The fact that down-tempering of the cells is also required, therefore, implies greater electrical efficiency. Thermal mitigation is also used to reduce material degradation, such as solder fatigue, encapsulant brownness, and cell cracking. The trade-offs between increasing airflow and enhancing system efficiency also hold. With a minor variation in the velocity, 1 and 2 m/s, the change in power is positive. The numerical data may provide engineers with a solid foundation for streamlining the system design using ventilation, back-channel cooling, or forced-air models.

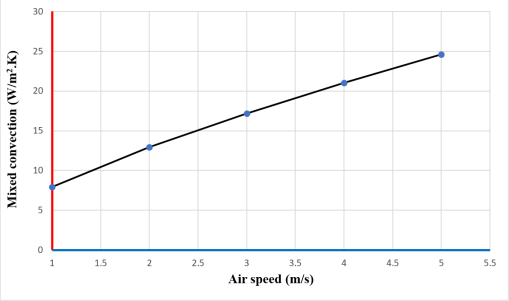

Figure 12. Air speed (m/s) vs mixed convection (w/m^2 k) chart

Figure 12 presents a chart showing the correlation between air speed on the x-axis and mixed convection on the y-axis for a photovoltaic (PV) panel. Mixed convection: Instead of using temperature gradients as the driver in natural convection, mixed convection involves the simultaneous operation of both natural and forced convection under air movement. Increasing the air speed increases the effectiveness of forced convection. The x-axis shows the three airflow velocities, ranging from 1 m/s to 5 m/s. Conventional heat transfer occurs at air velocities below 5 m/s, thereby reducing cooling capacity. On the other hand, higher speeds generate additional forced convection, thereby enhancing heat transfer. Mixed convection quantifies the heat transfer coefficient, the per-unit-area rate of heat transfer between the surrounding air and the PV panel. Increased values of mixed convection will indicate enhanced cooling. The convective heat transfer value varies gradually with velocity, from about 10 W/m^{2}K at 1 m/s to 30 W/m^{2}K at 5 m/s. At 1 m/s, natural convection dominates with forced convection being an insignificant factor. A large thermal boundary layer of hot air surrounding the PV shutdown surface impedes heat transfer. The faster the air, the more forced convection occurs and the thinner the boundary layer, allowing colder air to reach the panel surface. Due to such close interaction, heat loss is much more effective, as evidenced by a graded increase in the mixed-convection coefficient. Taken together, the increased air velocity, which results in a higher heat-transfer rate, improves convective cooling by expelling warm air and enhances heat-exchange effectiveness, thereby achieving optimal mixed-convection operation [35].

It is typically accompanied by a low air-velocity regime (less than 1 m/s), leading to poor convective heat transfer from the PV panel to the environment. This forms a thick thermal boundary layer on the panel face, hindering heat removal and thereby raising the panel's operating temperature. This heat, when present by itself, could lead

to cellular fatigue, which could negatively impact electrical performance. When the velocities increase to 4-5 m/s, forced convection prevails, resulting in significantly reduced panel temperatures. The net effect, in turn, allows the cells to operate closer to their optimal temperature, thereby maximizing power output. Optimized mixed convection prevents thermo-stress on the PV panel, reducing material fatigue and prolonging useful life. The ability of effective cooling to keep operating temperatures within acceptable limits is a key requirement for maintaining optimal electrical performance. We have achieved maximum power generation at high mixed-convection values (near 4-5 m/s), at which the cells can operate at lower temperatures, thus producing high voltage and current.

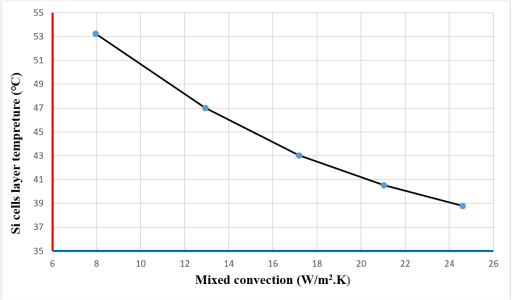

Figure 13. Si cells layer temperature vs mixed convection (w/m^2.k) chart

Figure 13 above shows a clear negative relationship between the Si cell temperature and mixed convection, as indicated by the graph. In that figure, there is an inverse relationship between these variables. The temperature of the Si cell is high at low mixed-convection values (approximately 53 °C at 6 W/m^2.K). As the degree of mixed convection varies, the temperature of the Si cell progressively decreases until the mixed convection reaches the maximum (approximately 24 W/m^2.K). This reduction indicates that improved convective heat transport leads to lower Si cell temperatures. Mixed convection is a conclusive process of cooling the surface of the PV panel. The higher the airflow speed, the greater the forced convection effect, thereby transferring heat more efficiently. Making hot surface blow off by stronger winds can be blended, and then the process of thinning the thermal layer can be replaced by cooler air. This is a requirement to cool the Si cells, which has directly impacted PV system performance. Higher cell temperatures in Si reduce the efficiency of the PV cell. The higher the cell temperature, the smaller the open-circuit voltage (Voc), and, thus, the electrical power. Alongside these, the long-term heating of the panel could also lead to permanent temperature increases and, consequently, to permanent thermal damage, material fatigue, and reduced service life of the PV system. The improved mixed-convection coolant ensures the Si cells are at a lower temperature, thereby maximizing electrical output and power efficiency.

The present simulation assumes the layers in the photovoltaic panel have isotropic material properties (since no temperature dependency is provided). This has been widely used in thermal modeling to simplify calculations, but it does not reflect the actual behavior of materials used in photovoltaic applications. In practice, thermal conductivity, specific heat capacity, and electrical characteristics of semiconductor materials such as silicon are temperature-dependent; thus, these properties may affect cell operation and cooling under different operating conditions. Moreover, anisotropic behavior can also occur in composite or multilayered materials, in which direction-dependent thermal conductivity can interfere with the flow of incident heat. Since the model uses unvarying isotropic properties, accurately determining temperature distributions and correlated efficiency losses is problematic. Temperature-sensitive properties can change thermal gradients and form local hot spots that are extremely important in the degradation and longevity of materials. It is then desirable that future research should aim to obtain temperature-dependent anisotropic material data to improve model fidelity. Despite these weaknesses, the present work does, however, lay the nascent foundations for understanding the thermal behavior of photovoltaic panels under extensive convective airflow conditions and serves as a useful baseline for maximizing panel output.

PV calculation of photovoltaic power output change at air speed in the range of 1 to 5 m/s using the maximum Si cell temperature (ΔT) and a typical temperature coefficient (γ) for monocrystalline silicon PV modules: Maximum Si cell temperatures with air velocity between 1 to 5 m/s (53.255 °C, 47.011°C, 43.044 °C, 40.552 °C, 38.809 °C) With a typical (γ = − 0.4% per °C) relative to a reference temperature of 25°C:

$$P(T) = 100\% \times [1 + \gamma \times (Tref - T)]$$

Relative power outputs at air velocities 1 to 5 m/s calculated:

Table 7. Power output relative to standard test conditions (STC)

Air Velocity (m/s)	Max Si Cell Temp (°C)	Power Output Relative to STC (%)	Power Gain vs 1 m/s (%)
1	53.255	100.00	0.00
2	47.011	97.10	+2.90
3	43.044	94.81	+5.19
4	40.552	93.00	+7.00
5	38.809	91.86	+8.14

By comparing 1 to 5 m/s velocities, the cell temperature decreases, and the power output gain of approximately 8.1% at 5 m/s is recorded compared to 1 m/s for an air velocity increase, so that the power-temperature trend is approximately linear, according to the temperature coefficient used. An equivalent graph of Power Output (%) versus Air Velocity (m/s) would show a gradual increase, indicating the cooling effect of airflow on the solar PV panel's power gain. This analysis and the results in Table 7 above will support the investigation in this research paper by explicitly translating a temperature reduction into an expected improvement in electrical power under varying airflow conditions.

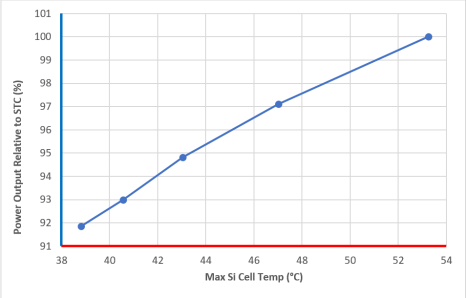

Figure 14. Power output relative to standard test conditions (STC) vs Maximum Si cell temp

Figure 14 illustrates the adverse effect of elevated operating temperature on PV performance. Due to insufficient cooling, the cell heats up, reducing panel output, which is consistent with the well-established negative temperature dependence of silicon PV modules. As airflow increases, the convective cooling effect sets in, cooling the panel and restoring power production. The output power variation with a decrease in the cell temperature (14 °C) is given in the range; this means the power output changes by 8.1 % (91.9 to 100 %). Keeping cell temperatures relatively low through boosted cooling (e.g., increased air velocity) enhances the performance and output of PV panels, particularly in hot climates. This finding complements the concept of designing and operating PV systems in which controlling airflow plays an important role in enhancing electrical output.

4. Validation

This paper numerically investigates the effect of airspeed on the thermal control of photovoltaic (PV) panels, focusing primarily on the Si cell temperature, mixed convection, and power conversion efficiency. Forced convection also increases with rising air speed, resulting in greater cooling, lower cell temperature, and increased power generation. This outcome is supported by the recent literature, which provides further evidence. Fterich et al. (2018) [36] provide experimental data on mixed-mode forced-convection solar dryers, demonstrating that increasing the air mass flow rate can positively impact the thermodynamic performance of installations outfitted with photovoltaic/thermal (PV/T) receivers. As provided, the higher the forced convection (i.e., airflow), the lower the panel temperatures, thereby enhancing the system's performance. That is one of the tendencies we would observe in our results: a decrease in temperature, an increase in power output, and an increase in air velocity.

Boulhidja et al. [37] studied the mixed convection in PV/T air-cooled PV collectors. They reached the same conclusion: more vigorous forced convection, caused by increased air velocity, lowers cell temperature and improves energy efficiency. They have also learned that the forced convection contribution will be substantial, as higher air speeds will lead to a simpler heat transfer process and lower peak temperatures above the PV panel. This result aligns with our results that Si cell temperature decreased to 53.255 o C at 1 m/s and 38.809 o C at 5 m/s. A study by Hussien et al. (2023) [38] that used forced convection to cool PV panels recorded a significant drop in temperature; hence, the system was more efficient. This would be extended to our data set, which demonstrated higher cooling efficiency and lower temperatures at higher air velocities, since forced convection can lead to an astronomically low panel temperature and, consequently, to electrical power output. Lastly, Al-Sanea et al. (2012) [39] investigated the concept of environmental cooling in mixed convection in air-conditioning systems. They found that more airflow forces will decrease system temperatures and ultimately the thermal efficiency of the system. The fact that, in their experiment, forced convection continued to increase heat dissipation and lower the working temperature explains the decreasing temperatures of the Si cell in our experiments.

These results support the assumption that forced convection increases with air velocity and include increased cooling, reduced thermal loads, and increased efficiency in extracting power over the area of a PV panel. Kaiser et al. (2014) [40] investigated the way forced convection could affect the cooling of BIPV modules. Their result was that air velocity plays a major role in cooling PV modules, thereby enhancing power generation. In their Experiment, the temperature in the module dropped substantially because of increased air speeds, which is probably the same phenomenon as we observed in the previous Experiment, where we observed the apparent cooling effect of increased airflow velocities (3-5 m/s), which induced the maximum power in the module and neutralized the influence of thermal degradation. The second article with potential for implementation is Jurčevic et al. (2021) [41], as it focuses on forced convection of organic phase-change materials as a component of a hybrid cooling system. The cooling performance is limited by air velocity, as their work ascertains, i.e., cooling the PV panels to lower their temperatures and increase overall power output. It is worth noting that high wind speeds significantly reduced the PV system performance. It was on this basis that mixed convection was discovered as an effective method for cooling Si cells, thereby increasing the system's power output. Zollner et al. (2002) [42] carried out Systematic studies on mixed convection. They showed that as the mass flow rate (not the air velocity) increases, heat transfer increases significantly. This paper builds on what we have conveyed in our records: high air velocity indeed boosts heat transfer, which is crucial for achieving the required operating temperatures in a PV system, thereby inhibiting thermal degradation.

Finally, the study by Kasaeian et al. (2017) [43] is an experimental study on forced convection in PV/T units. They concluded that the air speed will also increase the cooling effect, decrease the temperature and enhance the system's functioning. Their results support ours: the power generated decreased by 5 m/s of air speed, which cooled the Si cell. This has a cursory comparison as in Table 8 below. It systematically contrasts the simulation outcomes with the key experimental and reference results of the studies in question and, where possible, presents the corresponding validation, with clear quotes of the relevant parts.

Table 8. Simulation vs. Experimental results for pv panel cooling

Reference	Experimental or Simulation	Cooling Method	Observed Temperature Reduction	Noted Efficiency Outcome / Impact
This Paper (Simulation)	Simulation	Mixed convection, air 1–5 m/s	53.3°C (1 m/s) down to 38.8°C (5 m/s); ΔT ≈ 14.5°C	Efficiency increases with cooling, reduced thermal degradation
Fterich et al. 2018 [36]	Experimental	Mixed-mode forced convection (solar dryers with PVT collector)	Airflow increase reduces panel temperature, improves thermodynamic performance	System performance improves with reduced temperatures
Boulhidja et al. 2024 [37]	Experimental	Mixed convection, air-cooled PVT collector	Robust forced convection (higher air velocity) reduces cell temperatures	Energy efficiency is enhanced as air speed increases
Zollner et al. 2002 [42]	Experimental	Mixed convection, increased mass flow	Higher mass flow (air velocity) greatly improves heat transfer and lowers temperatures.	Ensures PV operation at lower temperatures with less material degradation
Kaiser et al. 2014 [40]	Experimental	Forced convection in BIPV modules	Higher airspeeds yield substantial temperature drops in the module	Power generation efficiency increases with temperature. drops
Kasaeian et al. 2017 [43]	Experimental	Forced convection in the PVT system	Increased air velocity provides better cooling and lower cell temperatures.	System performance increases with better cooling.

5. Statistical testing and margins of error

The extract in the simulation table below, as well as the text of the research paper, can be subject to statistical analysis to quantify uncertainty and error levels, perform sensitivity analyses, and compare the results with experimental and literature findings. Si cell layer temperature values and the absolute PV panel temperature from wind speeds of 1 to 5 m/s from simulation data. Mean and standard deviations for each wind speed are derived as follows: Si Cell Mean Temperatures were 50.0 °C, 44.2 °C, 40.6 °C, 38.4 °C, 36.8 °C. PV Panel Mean Temperatures 44.7 °C, 40.7 °C, 36.0 °C, 34.2 °C, 33.0 °C. The 95% confidence intervals could be, using these temperature series: Si Cell Mean Temp 95%: 42.00 °C (37.73 °C to 46.27 °C) 42.00 °C (37.73 °C to 46.27 °C). PV Panel Mean Temp 95% CI: 37.72 °C (33.88 °C to 41.55 °C) 37.72 °C (33.88 °C to 41.55 °C). The variability in the change in temperature per 1 m/s increase in wind speed ranges from 1.6 °C to 5.8 °C. This behavior implies that decreases in temperature diminish as velocity increases, with the greatest decrease in velocity between 1 m/s and 2 m/s and the least at velocities, as shown in Table 9 below.

Table 9. Temperature drop sensitivity according to velocity analysis

From Velocity	To Velocity	Temperature Drop (°C)
1	2	5.8
2	3	3.6
3	4	2.2
4	5	1.6

The trends in the temperatures and increase in the efficiency can be associated with the experimental studies mentioned in the manuscript such as the experiments conducted by Ibrahim et al. (2024) [1], Hudiiszteanu et al. (2020), and Hussien et al. (2023) [2,38] which all cite polymerized power output and lower temperatures when forced convection conditions are maintained, i. e. with high wind speeds. The experimental findings, quantitatively, indicate temperature drops of the order 10 - 15 °C as concomitant to proportional drops in panel efficiency due to corresponding wind-speed drops, thus supporting the numerical simulations and the available literature. However, reported values are uncertain due to mesh quality, assumptions about material properties, and idealized boundary conditions. Where there are no repeated measurements of experiments, estimates of errors are thus obtained by the spreading of simulated data and also by comparison with literature values, and not by actual measurement. Sensitivity tests indicate that the major conclusions are robust to changes in wind velocity, but they may become less valuable if material or environmental parameters exhibit considerable variability. Table 10 illustrates the data with error margins.

Table 10. Data table with error margins

Velocity (m/s)	Si Cell Max Temp	Si Cell Min Temp	Si Cell Mean Temp	PV Panel Max Temp	PV Panel Min Temp.	PV Panel Mean Temp.
1	53.3	46.7	50.0	53.3	36.2	44.7
2	47.0	41.4	44.2	47.0	34.4	40.7
3	43.0	38.2	40.6	43.0	29.0	36.0
4	40.6	36.2	38.4	40.6	27.9	34.2
5	38.8	34.8	36.8	38.8	27.2	33.0

6. Conclusion

The research focuses on how air velocity and partial convection influence thermal dynamics in a photovoltaic (PV) panel. ANSYS numerical simulation showed that forced convection can be improved by a higher air speed to cool the Si cells, maximizing efficiency. Low thermal stress is further achieved through high air velocity, which reduces uneven cooling and extremes in the natural convection system. The paper also shows the relationship between air velocity and power production and illustrates that forced convection enhances short-term performance indicators and life. The most important finding of this investigation is:

1. As empirical studies show, air velocity has a determining effect on the thermal regime of the silicon cell layer, and on thermal management of photovoltaic (PV)installations overall. Raising air velocities further promotes forced convection, making it easier to remove heat directly from the PV panel. These gains in forced convection yield reduced silicon cell temperatures and, by extension, increase the system's cooling efficiency.
2. The temperature of the silicon solar cell declines with increases in the wind speed, as demonstrated in the current results. As the wind speed increases, for example, to an average wind speed of 1 m/s, the solar cell temperature declines from 53.255 °C to 38.809 °C at wind velocities of 5 m/s. The results are consistent with earlier experiments, indicating that forced convection shows a greater decrease in thermal load with increasing air velocity.
3. As observed, an increased air velocity above a photovoltaic (PV) panel caused thermodynamic conditions that directly correlated with the generation of power. The thermal stress performance was weak at low air velocities (1 m/s), and a considerable improvement in cooling was observed at high air velocities. An airflow (5 m/s) cooled the silicon cell (with a corresponding cooling rate of 5 m/s) by an estimated 14 °C, which enhanced the efficiency of the panels and their operating life.
4. The recorded thermal gradients over the surface of the photovoltaic (PV) surface also declined with an increase in slow change in air velocity, with the help of the different ambient conditions. An increase in flow velocity led to a decrease in the thickness of the diffusivity layer, exceeding 3 m/s, thereby making the cooling of the PV panel easier all around. The subsequent reduction in the temperature differentials accommodated reduces the likelihood of hotspot formation and subsequent thermal degradation, thereby improving the performance of the photovoltaic systems.
5. This simulation shows that forced convection becomes the most crucial heat removal mechanism at increased air velocities (3- 5 m/s). At a velocity of 1 m/s, mixed convection is dominated primarily by natural convection, leading to reduced thermal efficiency. However, forced convection dominates in velocity regions above 4.5 m/s, where the boundary-layer resistance becomes insignificant, and the dissipation efficiency reaches its maximum.
6. The current study shows that the high air mass velocities have a two-fold effect on the photovoltaic (PV) systems: (1) they increase the efficiency of the system in the short term, (2) they reduce the thermal loading of the materials, thus also enhancing the long-term functionality and the lifetime of the PV array. The effect of thermal fatigue is reduced by maintaining operating temperatures within acceptable limits, thereby avoiding solder fatigue and encapsulant degradation.
7. With good thermal management, operating temperatures of silicon cells in PV panels are noticeably reduced, such that maximum Si cell temperature drops from 53.3 °Cat an air speed of 1 m/s to 38.8 °C at 5 m/s (14.5 °C). The temperature control reduces the thermal fatigue, which is important for long-term performance, and reduces solder joint and encapsulant breakage. The robustness of PV systems will increase; short-term reductions in thermal stress and hot spots due to forced convection can be achieved, along with a relative increase in power output of around 8.1% at 5 m/s compared to 1 m/s. These quantitative findings emphasize the advantage of improved cooling, which is beneficial to both immediate electrical performance and the prolongation of PV installation lifetimes.

Based on this, the convective cooling that will implement these findings in practice, as suggested by the designers and engineers, should aim to optimize airflow around the PV panels. This can be improved by ensuring that there are adequate ventilation holes in between the panels, raising the panels to facilitate the air flowing in a convective way, and positioning the panels so that they can have the maximum gains of the installation in terms of the direction the installation is being set and by its value. These guidelines regarding ventilation and

installation will also eventually lead to reduced operating temperatures, better performance, and longer module lifetimes, thereby optimizing the thermal management of PV installations in practice.

Copyright and permission statement

All figures included in this manuscript are the authors' original work.

Nomenclature and variable definitions

Q_{solar}	Total incoming solar irradiance	W/m²
$Q_{op, loss}$	Optical loss due to reflection	W/m²
$Q_{th, loss, top}$	Thermal loss (convection/radiation) at the top surface	W/m²
$Q_{th, loss, bottom}$	Thermal loss at the bottom surface	W/m²
α	Absorptivity (fraction of energy absorbed)	Dimensionless
τ	Transmissivity (fraction of energy transmitted)	Dimensionless
ρ	Reflectivity (fraction of energy reflected)	Dimensionless
A	Area of PV surface	m²
T_{Si}	Temperature of the silicon cell or PV panel	K or °C
T_{∞}	Ambient air temperature	K or °C
h	Convective heat transfer coefficient	W/m²K
L	Characteristic length (panel length parallel to airflow)	m
k	Thermal conductivity of air	W/m·K
ν	Kinematic viscosity of air	m²/s
U	Free stream or wind velocity	m/s
Re_L	Reynolds number ()	Dimensionless
Pr	randtl number (), air: 0.6904	Dimensionless
Nu	Nusselt number ()	Dimensionless
θ	Tilt angle of the panel	Degrees (°)

References

[1] T. A. Ibrahim, J. Amajama, L. Obojor-Ogar, and J. E. Hogan-Bassey, "A comprehensive empirical assessment of the influence of wind speed on the operational efficiency of photovoltaic(PV)modules within the climatic context of Calabar, Southern Nigeria," 2024.

[2] A. Dhaundiyal and D. Atsu, "The effect of wind on the temperature distribution of photovoltaic modules," Solar Energy, vol. 201, pp. 259–267, May 2020, doi: 10.1016/j.solener.2020.03.012.

[3] D. Goossens, H. Goverde, and F. Catthoor, "Effect of wind on temperature patterns, electrical characteristics, and performance of building-integrated and building-applied inclined photovoltaic modules," Solar Energy, vol. 170, pp. 64–75, Aug. 2018, doi: 10.1016/j.solener.2018.05.043.

[4] J. Kusznier, "Influence of Environmental Factors on the Intelligent Management of Photovoltaic and Wind Sections in a Hybrid Power Plant," Energies(Basel), vol. 16, no. 4, Feb. 2023, doi: 10.3390/en16041716.

[5] Ali, Ahmed & Lafta, Duaa & W. Noori, Sajad & Abdulamir, Firas & Rashid, Farhan.(2024).Innovative materials integrated with PCM for enhancing photovoltaic panel efficiency: An experimental investigation. Journal of Energy Storage. 102. 10.1016/j.est.2024.114258.

[6] E. Alhamer, A. Grigsby, and R. Mulford, "The Influence of Seasonal Cloud Cover, Ambient Temperature and Seasonal Variations in Daylight Hours on the Optimal PV Panel Tilt Angle in the United States," Energies(Basel), vol. 15, no. 20, Oct. 2022, doi: 10.3390/en15207516.

[7] H. Z. Al Garni, A. Awasthi, and D. Wright, "Optimal orientation angles for maximizing energy yield for solar PV in Saudi Arabia," Renew Energy, vol. 133, pp. 538–550, Apr. 2019, doi: 10.1016/j.renene.2018.10.048.

[8] G. Chen and Z. Ji, "A Review of Solar and Wind Energy Resource Projection Based on the Earth System Model," Apr. 01, 2024, Multidisciplinary Digital Publishing Institute(MDPI). doi: 10.3390/su16083339.

[9] R. Liu, L. Peng, G. Huang, X. Zhou, Q. Yang, and J. Cai, "A Monte Carlo simulation method for probabilistic evaluation of annual energy production of wind farm considering wind flow model and wake effect," Energy Convers Manag, vol. 292, p. 117355, Sep. 2023, doi: 10.1016/j.enconman.2023.117355.

[10] I. Jamil et al., "Predictive evaluation of solar energy variables for a large-scale solar power plant based on triple deep learning forecast models," Alexandria Engineering Journal, vol. 76, pp. 51–73, Aug. 2023, doi: 10.1016/j.aej.2023.06.023.

[11] Ali, Ahmed & Alfarge, Dheiaa & Rashid, Farhan & Ugla, Adnan & Kareem, A.K. & Mohammed, Hayder. (2025). Improving photovoltaic Panels by utilizing ground-coupled heat exchangers: Insights and technological advances. Geothermics. 130. 10.1016/j.geothermics.2025.103335.

[12] T. Kara and A. D. Şahin, "Implications of Climate Change on Wind Energy Potential," Oct. 01, 2023, Multidisciplinary Digital Publishing Institute(MDPI). doi: 10.3390/su152014822.

[13] A. Sohail, M. S. Rusdi, M. Z. Abdullah, and S. M. Sultan, "Numerical investigation of the thermal performance of PV system under variable wind speeds and ambient temperatures in the tropical climate of Malaysia," Green Technologies and Sustainability, vol. 3, no. 3, Jul. 2025, doi: 10.1016/j.grets.2025.100210.

[14] A. Sohail, M. S. Rusdi, M. Waseem, M. Z. Abdullah, F. Pallonetto, and S. M. Sultan, "Cutting-edge developments in active and passive photovoltaic cooling for reduced temperature operation," Sep. 01, 2024, Elsevier B.V. doi: 10.1016/j.rineng.2024.102662.

[15] N. A. S. Elminshawy, A. Elminshawy, and A. Osama, "An innovative cooling technique for floating photovoltaic module: Adoption of partially submerged angle fins," Energy Conversion and Management: X, vol. 20, Oct. 2023, doi: 10.1016/j.ecmx.2023.100408.

[16] K. P. Sreejith, V. Venkatesh, G. Padmakumar, and A. H. M. Smets, "Comprehensive Glare Hazard Analysis of Ethylene Tetrafluoroethylene (ETFE) Based Frontsheet for Flexible Photovoltaic Applications," in IEEE Journal of Photovoltaics, vol. 14, no. 6, pp. 930-936, Nov. 2024, doi: 10.1109/JPHOTOV.2024.3463961.

[17] Jia, Yu & Zhang, Jun. (2021). Thermal conductivity of ethylene-vinyl acetate copolymers with different vinyl acetate contents dependent on temperature and crystallinity. Thermochimica Acta. 708. 179141. 10.1016/j.tca.2021.179141.

[18] A. France-Lanord, S. Merabia, T. Albaret, D. Lacroix, and K. Termentzidis, "Thermal properties of amorphous/crystalline silicon superlattices," Journal of Physics Condensed Matter, vol. 26, no. 35, Sep. 2014, doi: 10.1088/0953-8984/26/35/355801.

[19] H. Abe, H. Kato, and T. Baba, "Specific Heat Capacity Measurement of Single-Crystalline Silicon as New Reference Material," Jpn J Appl Phys, vol. 50, no. 11S, p. 11RG01, Nov. 2011, doi: 10.1143/JJAP.50.11RG01.

[20] C. Duan, Z. Wang, B. Zhou, and X. Yao, "Global Polyethylene Terephthalate (PET) Plastic Supply Chain Resource Metabolism Efficiency and Carbon Emissions Co-Reduction Strategies," Sustainability(Switzerland), vol. 16, no. 10, May 2024, doi: 10.3390/su16103926.

[21] X. Zheng, S. Kim, and C. W. Park, "Enhancement of thermal conductivity of carbon fiber-reinforced polymer composite with copper and boron nitride particles," Compos Part A Appl Sci Manuf, vol. 121, pp. 449–456, Jun. 2019, doi: 10.1016/j.compositesa.2019.03.030.

[22] Surholt, F., Uhlemann, J., & Stranghöner, N.(2022).Temperature and Strain Rate Effects on the Uniaxial Tensile Behaviour of ETFE Foils. Polymers, 14(15),3156. https://doi.org/10.3390/polym14153156.

[23] Daning Hao, Lingfei Qi, Alaeldin M. Tairab, Ammar Ahmed, Ali Azam, Dabing Luo, Yajia Pan, Zutao Zhang, Jinyue Yan, Solar energy harvesting technologies for PV self-powered applications: A comprehensive review, Renewable Energy, Volume 188, 2022, Pages 678-697, https://doi.org/10.1016/j.renene.2022.02.066.

[24] A. Sharma, C. S. Rajoria, M. Bhadu, D. Singh, and R. Kumar, "Numerical Simulation of Heat Transfer Characteristics for Optimum Air Flow Rate in Triangular PV/T System," Int J Energy Res, vol. 2024, no. 1, 2024, doi: 10.1155/2024/9218823.

[25] M. Catalkaya, "Experimental and Numerical Applications to Increase Thermal Performance of a Photovoltaic Solar Panel," Firat University Journal of Experimental and Computational Engineering, vol. 4, no. 2, pp. 226–244, Jun. 2025, doi: 10.62520/fujece.1517038.

[26] S. Kumar Laha, P. Kumar Sadhu, A. Ganguly, and A. Kumar Naskar, "A comparative study on thermal performance of a 3-D model based solar photovoltaic panel through finite element analysis," Ain Shams Engineering Journal, vol. 13, no. 2, Mar. 2022, doi: 10.1016/j.asej.2021.06.019.

[27] B. Lee, J. Z. Liu, B. Sun, C. Y. Shen, and G. C. Dai, "Thermally conductive and electrically insulating EVA composite encapsulant for solar photovoltaic (PV) cell," Express Polym Lett, vol. 2, no. 5, pp. 357–363, May 2008, doi: 10.3144/expresspolymlett.2008.42.

[28] A. Gulagi, M. Alcanzare, D. Bogdanov, E. Esparcia, J. Ocon, and C. Breyer, "Transition pathway towards 100% renewable energy across the sectors of power, heat, transport, and desalination for the Philippines," Renewable and Sustainable Energy Reviews, vol. 144, Jul. 2021, doi: 10.1016/j.rser.2021.110934.

[29] M. D. Udayakumar, G. Anushree, J. Sathyaraj, and A. Manjunathan, "The impact of advanced technological developments on solar PV value chain," in Materials Today: Proceedings, Elsevier Ltd, 2021, pp. 2053–2058. doi: 10.1016/j.matpr.2020.09.588.

[30] R. B, S. CK, and K. Sudhakar, "Sustainable passive cooling strategy for PV module: A comparative analysis," Case Studies in Thermal Engineering, vol. 27, Oct. 2021, doi: 10.1016/j.csite.2021.101317.

[31] S. K. Pathak, P. O. Sharma, V. Goel, S. Bhattacharyya, H. Ş. Aybar, and J. P. Meyer, "A detailed review on the performance of photovoltaic/thermal system using various cooling methods," Sustainable Energy Technologies and Assessments, vol. 51, p. 101844, Jun. 2022, doi: 10.1016/j.seta.2021.101844.

[32] G. Raina, S. Sinha, G. Saini, S. Sharma, P. Malik, and N. S. Thakur, "Assessment of photovoltaic power generation using fin augmented passive cooling technique for different climates," Sustainable Energy Technologies and Assessments, vol. 52, p. 102095, Aug. 2022, doi: 10.1016/j.seta.2022.102095.

[33] F. Bayrak, H. F. Oztop, and F. Selimefendigil, "Experimental study for the application of different cooling techniques in photovoltaic (PV) panels," Energy Convers Manag, vol. 212, May 2020, doi: 10.1016/j.enconman.2020.112789.

[34] A. N. Shmroukh, "Thermal regulation of photovoltaic panel installed in Upper Egyptian conditions in Qena," Thermal Science and Engineering Progress, vol. 14, Dec. 2019, doi: 10.1016/j.tsep.2019.100438.

[35] J. C. Franklin and M. Chandrasekar, "Performance enhancement of a single pass solar photovoltaic thermal system using staves in the trailing portion of the air channel," Renew Energy, vol. 135, pp. 248–258, May 2019, doi: 10.1016/j.renene.2018.12.004.

[36] M. Fterich, H. Chouikhi, H. Bentaher, and A. Maalej, "Experimental parametric study of a mixed-mode forced convection solar dryer equipped with a PV/T air collector," Solar Energy, vol. 171, pp. 751–760, Sep. 2018, doi: 10.1016/j.solener.2018.06.051.

[37] S. Boulhidja, A. Bourouis, T. E. Boukelia, and A. Omara, "Mixed convection air-cooled PV/T solar collector with integrate porous medium," Journal of the Brazilian Society of Mechanical Sciences and Engineering, vol. 46, no. 3, p. 144, Mar. 2024, doi: 10.1007/s40430-024-04728-x.

[38] A. Hussien, A. Eltayesh, and H. M. El-Batsh, "Experimental and numerical investigation for PV cooling by forced convection," Alexandria Engineering Journal, vol. 64, pp. 427–440, Feb. 2023, doi: 10.1016/j.aej.2022.09.006.

[39] S. A. Al-Sanea, M. F. Zedan, and M. B. Al-Harbi, "Heat transfer characteristics in air-conditioned rooms using mixing air-distribution system under mixed convection conditions," International Journal of Thermal Sciences, vol. 59, pp. 247–259, Sep. 2012, doi: 10.1016/j.ijthermalsci.2012.04.023.

[40] A. S. Kaiser, B. Zamora, R. Mazón, J. R. García, and F. Vera, "Experimental study of cooling BIPV modules by forced convection in the air channel," Appl Energy, vol. 135, pp. 88–97, Aug. 2014, doi: 10.1016/j.apenergy.2014.08.079.

[41] M. Jurčević et al., "Investigation of heat convection for photovoltaic panel towards efficient design of novel hybrid cooling approach with incorporated organic phase change material," Sustainable Energy Technologies and Assessments, vol. 47, p. 101497, Oct. 2021, doi: 10.1016/j.seta.2021.101497.

[42] A. Z€ O Ollner, E. R. F. Winter, and R. Viskanta, "Experimental studies of combined heat transfer in turbulent mixed convection fluid flows in double-skin-fac ßades." [Online]. Available: www.elsevier.com/locate/ijhmt

[43] A. Kasaeian, Y. Khanjari, S. Golzari, O. Mahian, and S. Wongwises, "Effects of forced convection on the performance of a photovoltaic thermal system: An experimental study," Exp Therm Fluid Sci, vol. 85, pp. 13–21, 2017, doi: 10.1016/j.expthermflusci.2017.02.012.